

Relativistic Binary Systems and Gravitational Radiation

Contents

| | |
|--|-------------|
| 1. Topics | 1139 |
| 2. Participants | 1141 |
| 2.1. ICRANet participants | 1141 |
| 3. Brief description | 1143 |
| 4. Publications | 1147 |
| 5. APPENDICES | 1149 |
| A. Black Hole and Neutron Star Binaries: Theoretical Challenges | 1151 |
| A.1. Introduction | 1151 |
| A.2. Motion of binary pulsars in general relativity | 1152 |
| A.3. Timing of binary pulsars in general relativity | 1155 |
| A.4. Phenomenological approach to testing relativistic gravity with binary pulsar data | 1160 |
| A.5. Theory-space approach to testing relativistic gravity with bi- nary pulsar data | 1167 |
| A.5.1. Theory-space approaches to solar-system tests of rela- tivistic gravity | 1167 |
| A.5.2. Theory-space approaches to binary-pulsar tests of rela- tivistic gravity | 1168 |
| A.5.3. Tensor-scalar theories of gravity | 1170 |
| A.5.4. The role of the coupling function $a(\varphi)$; definition of the two-dimensional space of tensor-scalar gravity theories $T_1(\alpha_0, \beta_0)$ | 1174 |
| A.5.5. Tensor-scalar gravity, strong-field effects, and binary- pulsar observables | 1177 |
| A.5.6. Theory-space analyses of binary pulsar data | 1184 |
| A.6. Motion and radiation of binary black holes: post-Newtonian- expanded results | 1189 |
| A.7. Motion and radiation of binary black holes: the Effective One Body approach | 1191 |
| A.8. Conclusions | 1197 |
| Bibliography | 1199 |

1. Topics

- Effective-One-Body approach to the dynamics of binary black holes

2. Participants

2.1. ICRA Net participants

- T. Damour
- A. Nagar (INFN, Italy and IHES, France)

3. Brief description

The discovery, in our Galaxy, of binary systems comprising gravitationally condensed objects (neutron stars or black holes) has opened up both new experimental opportunities, and new theoretical challenges. The project discussed here concerns the *theoretical challenges* posed, for certain binary systems, by the necessity of getting a very accurate, general relativistic description of binary systems made of condensed objects. We have particularly in mind two different physical situations.

On the one hand, the discovery of binary pulsars in 1974 by Hulse and Taylor has given us the challenge of developing a theory of the relativistic motion of two compact objects which is accurate enough to match the remarkable precision of the observational data. Indeed, the very high stability of ‘pulsar clocks’ has made it possible to monitor the orbital dynamics of binary pulsars down to a precision allowing one to measure *secular* effects linked to very small ($\sim (v/c)^4$ and $\sim (v/c)^5$) terms in the orbital equations of motion, as well as *periodic* effects linked to $\mathcal{O}((v/c)^2)$ terms. An additional challenge is that these small ‘post-Newtonian-type’ terms in the equations of motion must be cleanly disentangled from the numerically much larger self-gravity effects. Indeed, though both types of effects can be formally expanded in a post-Newtonian (PN) expansion in powers of $1/c^2$, the self-gravity effects contain powers of $\gamma_i \equiv GM/(c^2R)$, where R denotes the *radius* of one of the compact objects, while the orbital effects should gather only the terms containing powers of $\gamma_e \equiv GM/(c^2D) \sim (v_{\text{orbital}}/c)^2$, where D denotes the typical *distance* separating the two objects. [The subscript i in γ_i refers to ‘internal’, by contrast to the subscript e which refers to ‘external’.] One can always consider γ_e as a small parameter (for instance $\gamma_e \sim 10^{-5}$ in the currently observed binary pulsars), while, because $R \ll D$, one will have $\gamma_i \gg \gamma_e$. For a usual star, or even a white dwarf, γ_i is quite small and can be used as an expansion parameter. By contrast, for a compact object (here defined as a neutron star or a black hole) γ_i will be of order unity, and cannot, *a priori*, be meaningfully used as an expansion parameter.

Special methods have been developed (notably by T. Damour) not only to show how one can, in principle, disentangle the ‘orbital’ (γ_e) expansion, from the ‘self-gravity’ (γ_i) one, but also to compute the γ_e expansion to the very high accuracy needed to discuss observational data. These methods were applied with success to the theory of the motion and timing of binary pulsars. The resulting relativistic “DD Timing Formula” has, since its derivation

many years ago, been of constant use by pulsar observers, and has crucially contributed to the data analysis of all the binary pulsars. In addition, it has allowed one to obtain the first accurate tests of Einstein's theory that probe the *strong-field aspects of relativistic gravity* (i.e. those which are potentially linked to physical effects linked to the strong internal self-gravity $\gamma_i \sim 1$ of compact objects). For a recent review, see (1).

The second physical situation which yields an even bigger theoretical challenge is the forthcoming detection of gravitational wave signals, in large interferometers (LIGO, VIRGO, GEO600, LISA, . . .). Indeed, one of the premier sources that one hopes to detect in LIGO/VIRGO is a coalescing binary black hole. The observationally important signal from these sources is generated during the last few orbits leading to a plunge and a merger. Though some aspects of this signal need three-dimensional numerical relativity simulations to be reliably computed, it can be argued that it is necessary to develop in parallel an *analytical description* of the motion of coalescing binary black holes down to the merger phase. A method of choice for such an analytical description is the '*effective one body*' approach to the motion of binary black holes (introduced a few years ago by A. Buonanno and T. Damour).

More precisely, for LIGO/VIRGO to successfully detect gravitational waves (GWs) from coalescing black hole binaries and to be able to reliably measure the source physical parameters, one needs to have in advance a large bank of "*templates*" that accurately represent the GW waveforms emitted by these binaries. The construction of faithful GW templates for coalescing binaries comprising spinning black holes (with arbitrary masses m_1, m_2 and spins $\mathbf{S}_1, \mathbf{S}_2$) poses a difficult challenge. Due to the multi-dimensionality of the corresponding parameter space, it seems impossible for state-of-the-art numerical simulations to densely sample this parameter space. This motivates the need to develop *analytical* methods for computing (as a function of the physical parameters $m_1, m_2, \mathbf{S}_1, \mathbf{S}_2$) the corresponding waveforms.

The Effective-One-Body (EOB) method (2; 3; 4; 5) was developed to analytically represent the motion of, and radiation from, coalescing binary black holes with arbitrary masses and spins. As early as 2000 (3) this method made several quantitative and qualitative predictions concerning the dynamics of the coalescence, and the corresponding waveform, notably: (i) a blurred transition from inspiral to a "plunge" that is just a smooth continuation of the inspiral, (ii) a sharp transition, around the merger of the black holes, between a continued inspiral and a ringdown signal, and (iii) estimates of the radiated energy and of the spin of the final black hole.

The recent impressive breakthroughs in numerical relativity (for a review see (6)) have given us access to extremely valuable, and reliable, information about the dynamics and radiation of binary black hole coalescence.

In addition, numerical simulations of test particles (with an added radiation reaction force) moving in black hole backgrounds have given an excellent

(and well controllable) “laboratory” for learning various ways of improving the EOB formalism by comparing it to numerical data (7). Let us recall in this respect that the analytical foundations of black hole perturbation theory have been laid long ago by Regge and Wheeler, and by Zerilli. Then, pioneering numerical studies of selected orbits (mainly circular or radial) led to the discovery of several important features of gravitational radiation in black hole backgrounds, such as the transition between the plunge signal and a ringing tail when a particle falls into a black hole (see the classic work of Davis, Ruffini and Tiomno (8)).

It is comforting (for theorists) to note that the picture which is emerging from the recent numerical simulations broadly confirms the predictions made by the EOB approach. This gives us confidence in the soundness of the various theoretical tools and assumptions used in this approach, such as the systematic use of *resummation* methods, notably Padé approximants.

In view of the recent progress in numerical relativity, the time is ripe for tapping the information present in numerical data, and for using it to “calibrate” in the best possible way the EOB approach (which contains various “flexibility parameters” linked to presently uncalculated high-order analytical effects). This general program has been initiated in a series of recent papers which used 3-dimensional numerical relativity results (9; 10; 11).

The current project feeds itself from three main sources of knowledge:

- information obtained from *numerical simulations* (both fully general relativistic ones, and the much simpler black hole perturbation ones);
- information obtained from high-accuracy *analytical perturbation theory* (notably post-Newtonian ones);
- the *Effective-One-Body approach* to the dynamics of binary black holes;
- the systematic use of various *resummation methods*, notably Padé approximants (12).

The project will explore the comparison between the analytical description of coalescing binary black holes (motion and radiation) and the recent numerical results on these systems (notably the high-accuracy numerical simulation of 15 orbits of an inspiralling equal-mass binary black hole system (13)). Some results have been recently obtained and published (10; 7; 14).

4. Publications

1. T. Damour, “Black Hole and Neutron Star Binaries: Theoretical Challenges”, arXiv:0705.3109 [gr-qc]. 53 pages, 3 eps figures, to appear in a revised edition of the book: Neutron Stars, Black Holes and Binary X-Ray Sources by H. Gursky and R. Ruffini

Some of the theoretical challenges posed by the general relativistic description of binary systems of compact objects (neutron stars or black holes) are reviewed. We recall the various ways one can use the theory of the motion, and of the timing, of binary pulsars to test the strong-field and/or radiative aspects of General Relativity. Recent advances in the theory of the motion and radiation of binary black holes are discussed. One emphasizes the usefulness of the Effective One Body approach in providing a quasi-analytical description of the waveform emitted by coalescing binary black holes.

2. T. Damour and A. Nagar, “Faithful Effective-One-Body waveforms of small-mass-ratio coalescing black-hole binaries”, Phys. Rev. D 76, 064028 (2007)

We address the problem of constructing high-accuracy, faithful analytic waveforms describing the gravitational wave signal emitted by inspiralling and coalescing binary black holes. We work within the Effective-One-Body (EOB) framework and propose a methodology for improving the current (waveform) implementations of this framework based on understanding, element by element, the physics behind each feature of the waveform, and on systematically comparing various EOB-based waveforms with “exact” waveforms obtained by numerical relativity approaches. The present paper focuses on small-mass-ratio non-spinning binary systems, which can be conveniently studied by Regge-Wheeler-Zerilli-type methods. Our results include: (i) a resummed, 3PN-accurate description of the inspiral waveform, (ii) a better description of radiation reaction during the plunge, (iii) a refined analytic expression for the plunge waveform, (iv) an improved treatment of the matching between the plunge and ring-down waveforms. This improved implementation of the EOB approach allows us to construct complete analytic waveforms which exhibit a remarkable agreement with the “exact” ones in modulus, frequency and phase. In particular, the analytic and numerical waveforms stay in phase, during the whole process, within $\pm 1.1\%$ of a cycle. We expect that the extension of our methodology to the comparable-mass case will be able to generate comparably accurate analytic waveforms of direct use for the ground-based network of

interferometric detectors of gravitational waves.

3. T. Damour and A. Nagar, “Final spin of a coalescing black-hole binary: an Effective-One-Body approach”, Phys. Rev. D 76, 044003 (2007)

We update the analytical estimate of the final spin of a coalescing black-hole binary derived within the Effective-One-Body (EOB) approach. We consider unequal-mass non-spinning black-hole binaries. It is found that a more complete account of relevant physical effects (higher post-Newtonian accuracy, ringdown losses) allows the *analytical* EOB estimate to ‘converge towards’ the recently obtained *numerical* results within 2%. This agreement illustrates the ability of the EOB approach to capture the essential physics of coalescing black-hole binaries. Our analytical approach allows one to estimate the final spin of the black hole formed by coalescing binaries in a mass range ($\nu = m_1 m_2 / (m_1 + m_2)^2 < 0.16$) which is not presently covered by numerical simulations.

4. T. Damour and A. Nagar, Comparing Effective-One-Body gravitational waveforms to accurate numerical data, arXiv:0711.2628

We continue the program of constructing, within the Effective-One-Body (EOB) approach, high accuracy, faithful analytic waveforms describing the gravitational wave signal emitted by inspiralling and coalescing binary black holes (BHs). We present the comparable-mass version of a new, resummed 3PN-accurate EOB quadrupolar waveform recently introduced in the small-mass-ratio limit. We compare the phase and the amplitude of this waveform to the recently published results of a high-accuracy numerical relativity (NR) simulation of 15 orbits of an inspiralling equal-mass binary BHs system performed by the Caltech-Cornell group. We find a remarkable agreement, both in phase and in amplitude, between the new EOB waveform and the published numerical data. More precisely: (i) in the gravitational wave (GW) frequency domain $M\omega < 0.08$ where the phase of one of the non-resummed “Taylor approximant” (T4) waveform matches well with the numerical relativity one, we find that the EOB phase fares as well, while (ii) for higher GW frequencies, $0.08 < M\omega \lesssim 0.14$, where the TaylorT4 approximant starts to significantly diverge from the NR phase, we show that the EOB phase continues to match well the NR one. We further propose various methods of tuning the two inspiral flexibility parameters, a_5 and v_{pole} , of the EOB waveform so as to “best fit” EOB predictions to numerical data. We find that the maximal dephasing between EOB and NR can then be reduced below 10^{-3} GW cycles over the entire span (30 GW cycles) of the simulation. Our resummed EOB amplitude agrees much better with the NR one than any of the previously considered non-resummed, post-Newtonian one.

5. APPENDICES

A. Black Hole and Neutron Star Binaries: Theoretical Challenges

A.1. Introduction

The discovery, in our Galaxy, of binary systems comprising gravitationally condensed objects (neutron stars or black holes) has opened up both new experimental opportunities, and new theoretical challenges. Here we shall focus on the *theoretical challenges* posed, for certain binary systems, by the necessity of getting a very accurate, general relativistic description of binary systems made of condensed objects. We have particularly in mind two different physical situations.

On the one hand, the discovery of binary pulsars in 1974 (15) has given us the challenge of developing a theory of the relativistic motion of two compact objects which is accurate enough to match the remarkable precision of the observational data. Indeed, the very high stability of ‘pulsar clocks’ has made it possible to monitor the orbital dynamics of binary pulsars down to a precision allowing one to measure *secular* effects linked to very small ($\sim (v/c)^4$ and $\sim (v/c)^5$) terms in the orbital equations of motion, as well as *periodic* effects linked to $\mathcal{O}((v/c)^2)$ terms. An additional challenge is that these small ‘post-Newtonian-type’ terms in the equations of motion must be cleanly disentangled from the numerically much larger self-gravity effects. Indeed, though both types of effects can be formally expanded in a post-Newtonian (PN) expansion in powers of $1/c^2$, the self-gravity effects contain powers of $\gamma_i \equiv GM/(c^2R)$, where R denotes the *radius* of one of the compact objects, while the orbital effects should gather only the terms containing powers of $\gamma_e \equiv GM/(c^2D) \sim (v_{\text{orbital}}/c)^2$, where D denotes the typical *distance* separating the two objects. [The subscript i in γ_i refers to ‘internal’, by contrast to the subscript e which refers to ‘external’.] One can always consider γ_e as a small parameter (for instance $\gamma_e \lesssim 10^{-5}$ in the currently observed binary pulsars), while, because $R \ll D$, one will have $\gamma_i \gg \gamma_e$. For a usual star, or even a white dwarf, γ_i is quite small and can be used as an expansion parameter. By contrast, for a compact object (here defined as a neutron star or a black hole) γ_i will be of order unity, and cannot, *a priori*, be meaningfully used as an expansion parameter. We shall review below some of the methods which have been used not only to show how one can, in principle, disentangle the ‘orbital’ (γ_e) expansion, from the ‘self-gravity’ (γ_i) one, but

also to compute the γ_e expansion to the very high accuracy needed to discuss observational data.

The second physical situation which yields an even bigger theoretical challenge is the forthcoming detection of gravitational wave signals, in large interferometers (LIGO, VIRGO, GEO600, LISA, . . .). Indeed, one of the premier sources that one hopes to detect in LIGO/VIRGO is a coalescing binary black hole. The observationally important signal for these sources is generated during the last few orbits leading to a plunge and a merger. Though some aspects of this signal need three-dimensional numerical relativity simulations to be reliably computed, we shall argue here for the need of developing in parallel an *analytical description* of the motion of coalescing binary black holes down to the merger phase. We shall present below an essential ingredient of such an analytical description: the ‘*effective one body*’ approach to the motion of binary black holes (16; 17).

A.2. Motion of binary pulsars in general relativity

The traditional (text book) approach to the problem of motion of N separate bodies in General Relativity (GR) consists of solving, by successive approximations, Einstein’s field equations (we use the signature $-+++$)

$$R_{\mu\nu} - \frac{1}{2} R g_{\mu\nu} = \frac{8\pi G}{c^4} T_{\mu\nu}, \quad (\text{A.2.1})$$

together with their consequence

$$\nabla_\nu T^{\mu\nu} = 0. \quad (\text{A.2.2})$$

To do so, one assumes some specific matter model, say a perfect fluid,

$$T^{\mu\nu} = (\varepsilon + p) u^\mu u^\nu + p g^{\mu\nu}. \quad (\text{A.2.3})$$

One expands (say in powers of Newton’s constant)

$$g_{\mu\nu}(x^\lambda) = \eta_{\mu\nu} + h_{\mu\nu}^{(1)} + h_{\mu\nu}^{(2)} + \dots, \quad (\text{A.2.4})$$

and uses the simplifications brought by the ‘Post-Newtonian’ approximation ($\partial_0 h_{\mu\nu} = c^{-1} \partial_t h_{\mu\nu} \ll \partial_i h_{\mu\nu}$; $v/c \ll 1$, $p \ll \varepsilon$). Then one integrates the local material equation of motion (A.2.2) over the volume of each separate body, labelled say by $a = 1, 2, \dots, N$. In so doing, one must define some ‘center of mass’ z_a^i of body a , as well as some (approximately conserved) ‘mass’ m_a of body a , together with some corresponding ‘spin vector’ S_a^i and, possibly, higher multipole moments.

An important feature of this traditional method is to use a *unique coordinate*

chart x^μ to describe the full N -body system. For instance, the center of mass, shape and spin of each body a are all described within this common coordinate system x^μ . This use of a single chart has several inconvenient aspects, even in the case of weakly self-gravitating bodies (as in the solar system case). Indeed, it means for instance that a body which is, say, spherically symmetric in its own ‘rest frame’ X^α will appear as deformed into some kind of ellipsoid in the common coordinate chart x^μ . Moreover, it is not clear how to construct ‘good definitions’ of the center of mass, spin vector, and higher multipole moments of body a , when described in the common coordinate chart x^μ . In addition, as we are interested in the motion of strongly self-gravitating bodies, it is not a priori justified to use a simple expansion of the type (A.2.4) because $h_{\mu\nu}^{(1)} \sim \sum_a Gm_a / (c^2 |\mathbf{x} - \mathbf{z}_a|)$ will not be uniformly small in the common coordinate system x^μ . It will be small if one stays far away from each object a , but, as recalled above, it will become of order unity on the surface of a compact body.

These two shortcomings of the traditional ‘one-chart’ approach to the relativistic problem of motion can be cured by using a ‘multi-chart’ approach. The multi-chart approach describes the motion of N (possibly, but not necessarily, compact) bodies by using $N + 1$ separate coordinate systems: (i) one *global* coordinate chart x^μ ($\mu = 0, 1, 2, 3$) used to describe the spacetime outside N ‘tubes’, each containing one body, and (ii) N *local* coordinate charts X_a^α ($\alpha = 0, 1, 2, 3$; $a = 1, 2, \dots, N$) used to describe the spacetime in and around each body a . The multi-chart approach was first used to discuss the motion of black holes and other compact objects (18; 19; 20; 21; 22; 23; 24; 25). Then it was also found to be very convenient for describing, with the high-accuracy required for dealing with modern technologies such as VLBI, systems of N weakly self-gravitating bodies, such as the solar system (26; 27).

The essential idea of the multi-chart approach is to combine the information contained in *several expansions*. One uses both a global expansion of the type (A.2.4) and several local expansions of the type

$$G_{\alpha\beta}(X_a^\gamma) = G_{\alpha\beta}^{(0)}(X_a^\gamma; m_a) + H_{\alpha\beta}^{(1)}(X_a^\gamma; m_a, m_b) + \dots, \quad (\text{A.2.5})$$

where $G_{\alpha\beta}^{(0)}(X; m_a)$ denotes the (possibly strong-field) metric generated by an isolated body of mass m_a (possibly with the additional effect of spin).

The separate expansions (A.2.4) and (A.2.5) are then ‘matched’ in some overlapping domain of common validity of the type $Gm_a/c^2 \lesssim R_a \ll |\mathbf{x} - \mathbf{z}_a| \ll D \sim |\mathbf{x}_a - \mathbf{x}_b|$ (with $b \neq a$), where one can relate the different coordinate systems by expansions of the form

$$x^\mu = z_a^\mu(T_a) + e_i^\mu(T_a) X_a^i + \frac{1}{2} f_{ij}^\mu(T_a) X_a^i X_a^j + \dots \quad (\text{A.2.6})$$

The multi-chart approach becomes simplified if one considers *compact* bodies (of radius R_a comparable to $2Gm_a/c^2$). In this case, it was shown (23), by considering how the ‘internal expansion’ (A.2.5) propagates into the ‘external’ one (A.2.4) via the matching (A.2.6), that, *in General Relativity*, the internal structure of each compact body was *effaced* to a very high degree, when seen in the external expansion (A.2.4). For instance, for non spinning bodies, the internal structure of each body (notably the way it responds to an external tidal excitation) shows up in the external problem of motion only at the *fifth post-Newtonian* (5PN) approximation, i.e. in terms of order $(v/c)^{10}$ in the equations of motion.

This ‘*effacement of internal structure*’ indicates that it should be possible to simplify the rigorous multi-chart approach by skeletonizing each compact body by means of some delta-function source. Mathematically, the use of distributional sources is delicate in a nonlinear theory such as GR. However, it was found that one can reproduce the results of the more rigorous matched-multi-chart approach by treating the divergent integrals generated by the use of delta-function sources by means of (complex) analytic continuation (23). The most efficient method (especially to high PN orders) has been found to use analytic continuation in the dimension of space d (28).

Finally, the most efficient way to derive the general relativistic equations of motion of N compact bodies consists of solving the equations derived from the action (where $g \equiv -\det(g_{\mu\nu})$)

$$S = \int \frac{d^{d+1}x}{c} \sqrt{g} \frac{c^4}{16\pi G} R(g) - \sum_a m_a c \int \sqrt{-g_{\mu\nu}(z_a^\lambda)} dz_a^\mu dz_a^\nu, \quad (\text{A.2.7})$$

formally using the standard weak-field expansion (A.2.4), but considering the space dimension d as an arbitrary complex number which is sent to its physical value $d = 3$ only at the end of the calculation. This ‘skeletonized’ effective action approach to the motion of compact bodies has been extended to other theories of gravity (21; 25). Finite-size corrections can be taken into account by adding nonminimal worldline couplings to the effective action (A.2.7) (29; 30).

Using this method¹ one has derived the equations of motion of *two* compact bodies at the 2.5PN (v^5/c^5) approximation level needed for describing binary pulsars (31; 32; 23):

$$\begin{aligned} \frac{d^2 z_a^i}{dt^2} &= A_{a0}^i(z_a - z_b) + c^{-2} A_{a2}^i(z_a - z_b, \mathbf{v}_a, \mathbf{v}_b) \\ &+ c^{-4} A_{a4}^i(z_a - z_b, \mathbf{v}_a, \mathbf{v}_b, \mathbf{S}_a, \mathbf{S}_b) \\ &+ c^{-5} A_{a5}^i(z_a - z_b, \mathbf{v}_a - \mathbf{v}_b) + \mathcal{O}(c^{-6}). \end{aligned} \quad (\text{A.2.8})$$

¹Or, more precisely, an essentially equivalent analytic continuation using the so-called ‘Riesz kernels’.

Here $A_{a0}^i = -Gm_b(z_a^i - z_b^i)/|z_a - z_b|^3$ denotes the Newtonian acceleration, A_{a2}^i its 1PN modification, A_{a4}^i its 2PN modification (together with the spin-orbit effects), and A_{a5}^i the 2.5PN contribution of order v^5/c^5 . [See the references above; or the review (33), for more references and the explicit expressions of A_2 , A_4 and A_5 .] It was verified that the term A_{a5}^i has the effect of decreasing the mechanical energy of the system by an amount equal (on average) to the energy lost in the form of gravitational wave flux at infinity. Note, however, that here A_{a5}^i was derived, in the near zone of the system, as a *direct* consequence of the general relativistic propagation of gravity, at the velocity c , between the two bodies. This highlights the fact that binary pulsar tests of the existence of A_{a5}^i are *direct tests of the reality of gravitational radiation*.

The 2.5PN equations of motion (A.2.8) are accurate enough for interpreting (together with the corresponding ‘timing formula’ discussed next) current and foreseeable binary pulsar data. In Section A.6 below we shall discuss recent improvements (3PN and 3.5PN) in the knowledge of the equations of motion and their use (in a suitably *resummed* form) for describing the last orbits of coalescing binary black holes.

A.3. Timing of binary pulsars in general relativity

In order to extract observational effects from the equations of motion (A.2.8) one needs to go through two steps: (i) to solve the equations of motion (A.2.8) so as to get the coordinate positions z_1 and z_2 as explicit functions of the coordinate time t , and (ii) to relate the coordinate motion $z_a(t)$ to the pulsar observables, i.e. mainly to the times of arrival of electromagnetic pulses on Earth.

The first step has been accomplished, in a form particularly useful for discussing pulsar timing, in Ref. (34). There (see also (35)) it was shown that, when considering the full (periodic and secular) effects of the $A_2 \sim v^2/c^2$ terms in Eq. (A.2.8), together with the secular effects of the $A_4 \sim v^4/c^4$ and $A_5 \sim v^5/c^5$ terms, the relativistic two-body motion could be written in a very simple ‘quasi-Keplerian’ form (in polar coordinates), namely:

$$\int n dt + \sigma = u - e_t \sin u, \quad (\text{A.3.1})$$

$$\theta - \theta_0 = (1 + k) 2 \arctan \left[\left(\frac{1 + e_\theta}{1 - e_\theta} \right)^{\frac{1}{2}} \tan \frac{u}{2} \right], \quad (\text{A.3.2})$$

$$R \equiv r_{ab} = a_R(1 - e_R \cos u), \quad (\text{A.3.3})$$

$$r_a \equiv |z_a - z_{CM}| = a_r(1 - e_r \cos u), \quad (\text{A.3.4})$$

$$r_b \equiv |z_b - z_{CM}| = a_{r'}(1 - e_{r'} \cos u). \quad (\text{A.3.5})$$

Here $n \equiv 2\pi/P_b$ denotes the orbital frequency, $k = \Delta\theta/2\pi = \langle\dot{\omega}\rangle/n = \langle\dot{\omega}\rangle P_b/2\pi$ the fractional periastron advance per orbit, u an auxiliary angle ('relativistic eccentric anomaly'), e_t, e_θ, e_R, e_r and $e_{r'}$ various 'relativistic eccentricities' and a_R, a_r and $a_{r'}$ some 'relativistic semi-major axes'. See (34) for the relations between these quantities, as well as their link to the relativistic energy and angular momentum E, J . A direct study (35) of the dynamical effect of the contribution $A_5 \sim v^5/c^5$ in the equations of motion (A.2.8) has checked that it led to a secular increase of the orbital frequency $n(t) \simeq n(0) + \dot{n}(t - t_0)$, and thereby to a quadratic term in the 'relativistic mean anomaly' $\ell = \int n dt + \sigma$ appearing on the left-hand side (L.H.S.) of Eq. (A.3.1):

$$\ell \simeq \sigma_0 + n_0(t - t_0) + \frac{1}{2} \dot{n}(t - t_0)^2. \quad (\text{A.3.6})$$

As for the contribution $A_4 \sim v^4/c^4$ it induces several secular effects in the orbital motion: various 2PN contributions to the dimensionless periastron parameter k ($\delta_4 k \sim v^4/c^4$ + spin-orbit effects), and secular variations in the inclination of the orbital plane (due to spin-orbit effects).

The second step in relating (A.2.8) to pulsar observations has been accomplished through the derivation of a '*relativistic timing formula*' (36; 37). The 'timing formula' of a binary pulsar is a multi-parameter mathematical function relating the observed time of arrival (at the radio-telescope) of the center of the N^{th} pulse to the integer N . It involves many different physical effects: (i) dispersion effects, (ii) travel time across the solar system, (iii) gravitational delay due to the Sun and the planets, (iv) time dilation effects between the time measured on the Earth and the solar-system-barycenter time, (v) variations in the travel time between the binary pulsar and the solar-system barycenter (due to relative accelerations, parallax and proper motion), (vi) time delays happening within the binary system. We shall focus here on the time delays which take place within the binary system. [See Refs. (38; 39) for the use of timing effects linked to parallax and proper motion.]

For a proper derivation of the time delays occurring within the binary system we need to use the multi-chart approach mentioned above. In the 'rest frame' ($X_a^0 = c T_a, X_a^i$) attached to the pulsar a , the pulsar phenomenon can be modelled by the secularly changing rotation of a beam of radio waves:

$$\Phi_a = \int \Omega_a(T_a) dT_a \simeq \Omega_a T_a + \frac{1}{2} \dot{\Omega}_a T_a^2 + \frac{1}{6} \ddot{\Omega}_a T_a^3 + \dots, \quad (\text{A.3.7})$$

where Φ_a is the longitude around the spin axis. [Depending on the precise definition of the rest-frame attached to the pulsar, the spin axis can either be fixed, or be slowly evolving, see e.g. (27).] One must then relate the initial direction (Θ_a, Φ_a) , and proper time T_a , of emission of the pulsar beam to the coordinate direction and coordinate time of the null geodesic representing the electromagnetic beam in the 'global' coordinates x^μ used to describe the

dynamics of the binary system [NB: the explicit orbital motion (A.3.1)–(A.3.5) refers to such global coordinates $x^0 = ct, x^i$]. This is done by using the link (A.2.6) in which z_a^i denotes the global coordinates of the ‘center of mass’ of the pulsar, T_a the local (proper) time of the pulsar frame, and where, for instance

$$e_i^0 = \frac{v_i}{c} \left(1 + \frac{1}{2} \frac{v^2}{c^2} + 3 \frac{Gm_b}{c^2 r_{ab}} + \dots \right) + \dots \quad (\text{A.3.8})$$

Using the link (A.2.6) (with expressions such as (A.3.8) for the coefficients e_i^μ, \dots) one finds, among other results, that a radio beam emitted in the proper direction N^i in the local frame appears to propagate, in the global frame, in the coordinate direction n^i where

$$n^i = N^i + \frac{v^i}{c} - N^j \frac{N^j v^j}{c} + \mathcal{O} \left(\frac{v^2}{c^2} \right). \quad (\text{A.3.9})$$

This is the well known ‘aberration effect’, which will then contribute to the timing formula.

One must also write the link between the pulsar ‘proper time’ T_a and the coordinate time $t = x^0/c = z_a^0/c$ used in the orbital motion (A.3.1)–(A.3.5). This reads

$$-c^2 dT_a^2 = \tilde{g}_{\mu\nu}(a^\lambda) dz_a^\mu dz_a^\nu \quad (\text{A.3.10})$$

where the ‘tilde’ denotes the operation consisting (in the matching approach) in discarding in $g_{\mu\nu}$ the ‘self contributions’ $\sim (Gm_a/R_a)^n$, while keeping the effect of the companion ($\sim Gm_b/r_{ab}$, etc. . .). One checks that this is equivalent (in the dimensional-continuation approach) to taking $x^\mu = z_a^\mu$ for sufficiently *small* values of the real part of the dimension d . To lowest order this yields the link

$$T_a \simeq \int dt \left(1 - \frac{2Gm_b}{c^2 r_{ab}} - \frac{v_a^2}{c^2} \right)^{\frac{1}{2}} \simeq \int dt \left(1 - \frac{Gm_b}{c^2 r_{ab}} - \frac{1}{2} \frac{v_a^2}{c^2} \right) \quad (\text{A.3.11})$$

which combines the special relativistic and general relativistic time dilation effects. Hence, following (37) we can refer to them as the ‘Einstein time delay’.

Then, one must compute the (global) time taken by a light beam emitted by the pulsar, at the proper time T_a (linked to t_{emission} by (A.3.11)), in the initial global direction n^i (see Eq. (A.3.9)), to reach the barycenter of the solar system. This is done by writing that this light beam follows a null geodesic: in particular

$$0 = ds^2 = g_{\mu\nu}(x^\lambda) dx^\mu dx^\nu \simeq - \left(1 - \frac{2U}{c^2} \right) c^2 dt^2 + \left(1 + \frac{2U}{c^2} \right) dx^2 \quad (\text{A.3.12})$$

where $U = Gm_a/|\mathbf{x} - \mathbf{z}_a| + Gm_b/|\mathbf{x} - \mathbf{z}_b|$ is the Newtonian potential within the binary system. This yields (with $t_e \equiv t_{\text{emission}}, t_a \equiv t_{\text{arrival}}$)

$$t_a - t_e = \int_{t_e}^{t_a} dt \simeq \frac{1}{c} \int_{t_e}^{t_a} |d\mathbf{x}| + \frac{2}{c^3} \int_{t_e}^{t_a} \left(\frac{Gm_a}{|\mathbf{x} - \mathbf{z}_a|} + \frac{Gm_b}{|\mathbf{x} - \mathbf{z}_b|} \right) |d\mathbf{x}|. \quad (\text{A.3.13})$$

The first term on the last RHS of Eq. (A.3.13) is the usual ‘light crossing time’ $\frac{1}{c} |z_{\text{barycenter}}(t_a) - z_a(t_e)|$ between the pulsar and the solar barycenter. It contains the ‘Roemer time delay’ due to the fact that $z_a(t_e)$ moves on an orbit. The second term on the last RHS of Eq. (A.3.13) is the ‘Shapiro time delay’ due to the propagation of the beam in a curved spacetime (only the Gm_b piece linked to the companion is variable). For a discussion of the $\mathcal{O}(v/c)$ fractional corrections to the Shapiro time delay see (40) and references therein.

When inserting the ‘quasi-Keplerian’ form (A.3.1)–(A.3.5) of the relativistic motion in the ‘Roemer’ term in (A.3.13), together with all other relativistic effects, one finds that the final expression for the relativistic timing formula can be significantly simplified by doing two mathematical transformations. One can redefine the ‘time eccentricity’ e_t appearing in the ‘Kepler equation’ (A.3.1), and one can define a new ‘eccentric anomaly’ angle: $u \rightarrow u^{\text{new}}$ [we henceforth drop the superscript ‘new’ on u]. After these changes, the binary-system part of the general relativistic timing formula (37) takes the form (we suppress the index a on the pulsar proper time T_a)

$$t_{\text{barycenter}} - t_0 = D^{-1}[T + \Delta_R(T) + \Delta_E(T) + \Delta_S(T) + \Delta_A(T)] \quad (\text{A.3.14})$$

with

$$\Delta_R = x \sin \omega [\cos u - e(1 + \delta_r)] + x[1 - e^2(1 + \delta_\theta)^2]^{1/2} \cos \omega \sin u \quad (\text{A.3.15})$$

$$\Delta_E = \gamma \sin u, \quad (\text{A.3.16})$$

$$\Delta_S = -2r \ln\{1 - e \cos u - s[\sin \omega (\cos u - e) + (1 - e^2)^{1/2} \cos \omega \sin u]\} \quad (\text{A.3.17})$$

$$\Delta_A = A\{\sin[\omega + A_e(u)] + e \sin \omega\} + B\{\cos[\omega + A_e(u)] + e \cos \omega\} \quad (\text{A.3.18})$$

where $x = x_0 + \dot{x}(T - T_0)$ represents the projected light-crossing time ($x = a_{\text{pulsar}} \sin i/c$), $e = e_0 + \dot{e}(T - T_0)$ a certain (relativistically-defined) ‘timing eccentricity’, $A_e(u)$ the function

$$A_e(u) \equiv 2 \arctan \left[\left(\frac{1+e}{1-e} \right)^{1/2} \tan \frac{u}{2} \right], \quad (\text{A.3.19})$$

$\omega = \omega_0 + k A_e(u)$ the ‘argument of the periastron’, and where the (relativistically-defined) ‘eccentric anomaly’ u is the function of the ‘pulsar proper time’

T obtained by solving the Kepler equation

$$u - e \sin u = 2\pi \left[\frac{T - T_0}{P_b} - \frac{1}{2} \dot{P}_b \left(\frac{T - T_0}{P_b} \right)^2 \right]. \quad (\text{A.3.20})$$

It is understood here that the pulsar proper time T corresponding to the N^{th} pulse is related to the integer N by an equation of the form

$$N = c_0 + \nu_p T + \frac{1}{2} \dot{\nu}_p T^2 + \frac{1}{6} \ddot{\nu}_p T^3. \quad (\text{A.3.21})$$

From these formulas, one sees that δ_θ (and δ_r) measure some relativistic distortion of the pulsar orbit, γ the amplitude of the ‘Einstein time delay’² Δ_E , and r and s the *range* and *shape* of the ‘Shapiro time delay’³ Δ_S . Note also that the dimensionless PPK parameter k measures the *non-uniform* advance of the periastron. It is related to the often quoted *secular* rate of periastron advance $\dot{\omega} \equiv \langle d\omega/dt \rangle$ by the relation $k = \dot{\omega} P_b / 2\pi$. It has been explicitly checked that binary-pulsar observational data do indeed require to model the relativistic periastron advance by means of the non-uniform (and non-trivial) function of u multiplying k on the R.H.S. of Eq. (A.3.19) (41)⁴. Finally, we see from Eq. (A.3.20) that P_b represents the (periastron to periastron) orbital period at the fiducial epoch T_0 , while the dimensionless parameter \dot{P}_b represents the time derivative of P_b (at T_0).

Schematically, the structure of the DD timing formula (A.3.14) is

$$t_{\text{barycenter}} - t_0 = F [T_N; \{p^K\}; \{p^{PK}\}; \{q^{PK}\}], \quad (\text{A.3.22})$$

where $t_{\text{barycenter}}$ denotes the solar-system barycentric (infinite frequency) arrival time of a pulse, T the pulsar emission proper time (corrected for aberration), $\{p^K\} = \{P_b, T_0, e_0, \omega_0, x_0\}$ is the set of *Keplerian* parameters, $\{p^{PK} = k, \gamma, \dot{P}_b, r, s, \delta_\theta, \dot{e}, \dot{x}\}$ the set of *separately measurable post-Keplerian* parameters, and $\{q^{PK}\} = \{\delta_r, A, B, D\}$ the set of *not separately measurable post-Keplerian* parameters (41). [The parameter D is a ‘Doppler factor’ which enters as an overall multiplicative factor D^{-1} on the right-hand side of Eq. (A.3.14).]

A further simplification of the DD timing formula was found possible. Indeed, the fact that the parameters $\{q^{PK}\} = \{\delta_r, A, B, D\}$ are not separately measurable means that they can be absorbed in changes of the other param-

²The post-Keplerian timing parameter γ , first introduced in (36), has the dimension of time, and should not be confused with the dimensionless post-Newtonian Eddington parameter γ^{PPN} probed by solar-system experiments (see below).

³The dimensionless parameter s is numerically equal to the sine of the inclination angle i of the orbital plane, but its real definition within the PPK formalism is the timing parameter which determines the ‘shape’ of the logarithmic time delay $\Delta_S(T)$.

⁴Alas this function is theory-independent, so that the non-uniform aspect of the periastron advance cannot be used to yield discriminating tests of relativistic gravity theories.

eters. The explicit formulas for doing that were given in (37) and (41): they consist in redefining e, x, P_b, δ_θ and δ_r . At the end of the day, it suffices to consider a simplified timing formula where $\{\delta_r, A, B, D\}$ have been set to some given fiducial values, e.g. $\{0, 0, 0, 1\}$, and where one only fits for the remaining parameters $\{p^K\}$ and $\{p^{PK}\}$.

Finally, let us mention that it is possible to extend the general parametrized timing formula (A.3.22) by writing a similar parametrized formula describing the effect of the pulsar orbital motion on the directional spectral luminosity [$d(\text{energy}) / d(\text{time}) d(\text{frequency}) d(\text{solid angle})$] received by an observer. As discussed in detail in (41) this introduces a new set of ‘pulse-structure post-Keplerian parameters’.

A.4. Phenomenological approach to testing relativistic gravity with binary pulsar data

As said in the Introduction, binary pulsars contain strong gravity domains and should therefore allow one to test the strong-field aspects of relativistic gravity. The question we face is then the following: How can one use binary pulsar data to test strong-field (and radiative) gravity?

Two different types of answers can be given to this question: a *phenomenological* (or *theory-independent*) one, or various types of *theory-dependent* approaches. In this Section we shall consider the phenomenological approach.

The phenomenological approach to binary-pulsar tests of relativistic gravity is called the *parametrized post-Keplerian formalism* (42; 41). This approach is based on the fact that the mathematical form of the multi-parameter DD timing formula (A.3.22) was found to be applicable not only in General Relativity, but also in a wide class of alternative theories of gravity. Indeed, any theory in which gravity is mediated not only by a metric field $g_{\mu\nu}$ but by a general combination of a metric field and of one or several scalar fields $\varphi^{(a)}$ will induce relativistic timing effects in binary pulsars which can still be parametrized by the formulas (A.3.14)–(A.3.21). Such general ‘tensor-multi-scalar’ theories of gravity contain arbitrary functions of the scalar fields. They have been studied in full generality in (43). It was shown that, under certain conditions, such tensor-scalar gravity theories could lead, because of strong-field effects, to very different predictions from those of General Relativity in binary pulsar timing observations (44; 45; 29). However, the point which is important for this Section, is that even when such strong-field effects develop one can still use the universal DD timing formula (A.3.22) to fit the observed pulsar times of arrival.

The basic idea of the phenomenological, parametrized post-Keplerian (PPK) approach is then the following: By least-square fitting the observed sequence of pulsar arrival times t_N to the parametrized formula (A.3.22) (in which T_N is

defined by Eq. (A.3.21) which introduces the further parameters $\nu_p, \dot{\nu}_p, \ddot{\nu}_p$ one can phenomenologically extract from raw observational data the (best fit) values of all the parameters entering Eqs. (A.3.21) and (A.3.22). In particular, one so determines both the set of Keplerian parameters $\{p^K\} = \{P_b, T_0, e_0, \omega_0, x_0\}$, and the set of post-Keplerian (PK) parameters $\{p^{PK}\} = \{k, \gamma, \dot{P}_b, r, s, \delta_\theta, \dot{e}, \dot{x}\}$. In extracting these values, we did not have to assume any theory of gravity. However, each specific theory of gravity will make specific predictions relating the PK parameters to the Keplerian ones, and to the two (a priori unknown) masses m_a and m_b of the pulsar and its companion. [For certain PK parameters one must also consider other variables related to the spin vectors of a and b .] In other words, the measurement (in addition of the Keplerian parameters) of each PK parameter defines, for each given theory, a *curve in the (m_a, m_b) mass plane*. For any given theory, the measurement of two PK parameters determines two curves and thereby generically determines the values of the two masses m_a and m_b (as the point of intersection of these two curves). Therefore, as soon as one measures *three* PK parameters one obtains a *test* of the considered gravity theory. The test is passed only if the three curves meet at one point. More generally, the measurement of n PK timing parameters yields $n - 2$ independent tests of relativistic gravity. Any one of these tests, i.e. any simultaneous measurement of three PK parameters can either confirm or put in doubt any given theory of gravity.

As General Relativity is our current most successful theory of gravity, it is clearly the prime target for these tests. We have seen above that the timing data of each binary pulsar provides a maximum of 8 PK parameters: $k, \gamma, \dot{P}_b, r, s, \delta_\theta, \dot{e}$ and \dot{x} . Here, we were talking about a normal ‘single line’ binary pulsar where, among the two compact objects a and b only one of the two, say a is observed as a pulsar. In this case, one binary system can provide up to $8 - 2 = 6$ tests of GR. In practice, however, it has not yet been possible to measure the parameter δ_θ (which measures a small relativistic deformation of the elliptical orbit), nor the secular parameters \dot{e} and \dot{x} . The original Hulse-Taylor system PSR 1913+16 has allowed one to measure 3 PK parameters: $k \equiv \langle \dot{\omega} \rangle P_b / 2\pi$, γ and \dot{P}_b . The two parameters k and γ involve (non radiative) strong-field effects, while, as explained above, the orbital period derivative \dot{P}_b is a direct consequence of the term $A_5 \sim v^5/c^5$ in the binary-system equations of motion (A.2.5). The term A_5 is itself directly linked to the retarded propagation, at the velocity of light, of the gravitational interaction between the two strongly self-gravitating bodies a and b . Therefore, any test involving \dot{P}_b will be a *mixed radiative strong-field* test.

Let us explain on this example what information one needs to implement a phenomenological test such as the $(k - \gamma - \dot{P}_b)_{1913+16}$ one. First, we need to know the predictions made by the considered target theory for the PK parameters k, γ and \dot{P}_b as functions of the two masses m_a and m_b . These predictions have been worked out, for General Relativity, in Refs. (36; 35; 37).

Introducing the notation (where $n \equiv 2\pi/P_b$)

$$M \equiv m_a + m_b \quad (\text{A.4.1})$$

$$X_a \equiv m_a/M; \quad X_b \equiv m_b/M; \quad X_a + X_b \equiv 1 \quad (\text{A.4.2})$$

$$\beta_O(M) \equiv \left(\frac{GMn}{c^3} \right)^{1/3}, \quad (\text{A.4.3})$$

they read

$$k^{\text{GR}}(m_a, m_b) = \frac{3}{1-e^2} \beta_O^2, \quad (\text{A.4.4})$$

$$\gamma^{\text{GR}}(m_a, m_b) = \frac{e}{n} X_b(1+X_b) \beta_O^2, \quad (\text{A.4.5})$$

$$\dot{P}_b^{\text{GR}}(m_a, m_b) = -\frac{192\pi}{5} \frac{1 + \frac{73}{24}e^2 + \frac{37}{96}e^4}{(1-e^2)^{7/2}} X_a X_b \beta_O^5. \quad (\text{A.4.6})$$

However, if we use the three predictions (A.4.4)–(A.4.6), together with the best current observed values of the PK parameters $k^{\text{obs}}, \gamma^{\text{obs}}, \dot{P}_b^{\text{obs}}$ (46) we shall find that the three curves $k^{\text{GR}}(m_a, m_b) = k^{\text{obs}}, \gamma^{\text{GR}}(m_a, m_b) = \gamma^{\text{obs}}, \dot{P}_b^{\text{GR}}(m_a, m_b) = \dot{P}_b^{\text{obs}}$ in the (m_a, m_b) mass plane *fail to meet* at about the 13σ level! Should this put in doubt General Relativity? No, because Ref. (47) has shown that the time variation (notably due to galactic acceleration effects) of the Doppler factor D entering Eq. (A.3.14) entailed an extra contribution to the ‘observed’ period derivative \dot{P}_b^{obs} . We need to subtract this non-GR contribution before drawing the corresponding curve: $\dot{P}_b^{\text{GR}}(m_a, m_b) = \dot{P}_b^{\text{obs}} - \dot{P}_b^{\text{galactic}}$. Then one finds that the three curves *do meet* within one σ . This yields a deep confirmation of General Relativity, and a direct observational proof of the reality of gravitational radiation.

We said several times that this test is also a probe of the strong-field aspects of GR. How can one see this? A look at the GR predictions (A.4.4)–(A.4.6) does not exhibit explicit strong-field effects. Indeed, the derivation of Eqs. (A.4.4)–(A.4.6) used in a crucial way the ‘effacement of internal structure’ that occurs in the general relativistic dynamics of compact objects. This non trivial property is rather specific of GR and means that, in this theory, all the strong-field effects can be *absorbed* in the definition of the masses m_a and m_b . One can, however, verify that strong-field effects do enter the observable PK parameters k, γ, \dot{P}_b etc. . . by considering how the theoretical predictions (A.4.4)–(A.4.6) get modified in alternative theories of gravity. The presence of such strong-field effects in PK parameters was first pointed out in Ref. (21) (see also (48)) for the Jordan-Fierz-Brans-Dicke theory of gravity, and in Ref. (22) for Rosen’s bi-metric theory of gravity. A detailed study of such strong-field deviations was then performed in (43; 44; 45) for general tensor-(multi)-scalar theories of gravity. In the following Section we shall

exhibit how such strong-field effects enter the various post-Keplerian parameters.

Continuing our historical review of phenomenological pulsar tests, let us come to the binary system which was the first one to provide several ‘pure strong-field tests’ of relativistic gravity, without mixing of radiative effects: PSR 1534+12. In this system, it was possible to measure the four (non radiative) PK parameters k, γ, r and s . [We see from Eq. (A.3.17) that r and s measure, respectively, the *range* and the *shape* of the ‘Shapiro time delay’ Δ_S .] The measurement of the 4 PK parameters k, γ, r, s define 4 curves in the (m_a, m_b) mass plane, and thereby yield 2 strong-field tests of GR. It was found in (49) that GR passes these two tests. For instance, the ratio between the measured value s^{obs} of the phenomenological parameter⁵ s and the value $s^{\text{GR}}[k^{\text{obs}}, \gamma^{\text{obs}}]$ predicted by GR on the basis of the measurements of the two PK parameters k and γ (which determine, via Eqs. (A.4.4), (A.4.5), the GR-predicted value of m_a and m_b) was found to be $s^{\text{obs}}/s^{\text{GR}}[k^{\text{obs}}, \gamma^{\text{obs}}] = 1.004 \pm 0.007$ (49). The most recent data (50) yield $s^{\text{obs}}/s^{\text{GR}}[k^{\text{obs}}, \gamma^{\text{obs}}] = 1.000 \pm 0.007$. We see that we have here a confirmation of the strong-field regime of GR at the 1% level.

Another way to get phenomenological tests of the strong field aspects of gravity concerns the possibility of a violation of the strong equivalence principle. This is parametrized by phenomenologically assuming that the ratio between the gravitational and the inertial mass of the pulsar differs from unity (which is its value in GR): $(m_{\text{grav}}/m_{\text{inert}})_a = 1 + \Delta_a$. Similarly to what happens in the Earth-Moon-Sun system (51), the three-body system made of a binary pulsar and of the Galaxy exhibits a ‘polarization’ of the orbit which is proportional to $\Delta \equiv \Delta_a - \Delta_b$, and which can be constrained by considering certain quasi-circular neutron-star-white-dwarf binary systems (52). See (53) for recently published improved limits⁶ on the phenomenological equivalence-principle violation parameter Δ .

The Parkes multibeam survey has recently discovered several new interesting ‘relativistic’ binary pulsars, thereby giving a huge increase in the number of phenomenological tests of relativistic gravity. Among those new binary pulsar systems, two stand out as superb testing grounds for relativistic gravity: (i) PSR J1141–6545 (55; 56), and (ii) the remarkable double binary pulsar PSR J0737–3039A and B (57; 58; 59; 60).

The PSR J1141–6545 timing data have led to the measurement of 3 PK parameters: k, γ , and \dot{P}_b (56). As in PSR 1913+16 this yields one mixed

⁵As already mentioned the dimensionless parameter s is numerically equal (in all theories) to the sine of the inclination angle i of the orbital plane, but it is better thought, in the PPK formalism, as a phenomenological timing parameter determining the ‘shape’ of the logarithmic time delay $\Delta_S(T)$.

⁶Note, however, that these limits, as well as those previously obtained in (54), assume that the (a priori pulsar-mass dependent) parameter $\Delta \simeq \Delta_a$ is the same for all the analyzed pulsars.

radiative-strong-field test⁷.

The timing data of the millisecond binary pulsar PSR J0737–3039A have led to the direct measurement of 5 PK parameters: k, γ, r, s and \dot{P}_b (58; 59; 60). In addition, the ‘double line’ nature of this binary system (i.e. the fact that one observes both components, A and B , as radio pulsars) allows one to perform new phenomenological tests by using *Keplerian* parameters. Indeed, the simultaneous measurement of the Keplerian parameters x_a and x_b representing the projected light crossing times of both pulsars (A and B) gives access to the combined Keplerian parameter

$$R^{\text{obs}} \equiv \frac{x_b^{\text{obs}}}{x_a^{\text{obs}}}. \quad (\text{A.4.7})$$

On the other hand, the general derivation of (37) (applicable to any Lorentz-invariant theory of gravity, and notably to any tensor-scalar theory) shows that the theoretical prediction for the the ratio R , considered as a function of the masses m_a and m_b , is

$$R^{\text{theory}} = \frac{m_a}{m_b} + \mathcal{O}\left(\frac{v^4}{c^4}\right). \quad (\text{A.4.8})$$

The absence of any *explicit* strong-field-gravity effects in the theoretical prediction (A.4.8) (to be contrasted, for instance, with the predictions for PK parameters in tensor-scalar gravity discussed in the next Section) is mainly due to the convention used in (37) and (41) for *defining* the masses m_a and m_b . These are always defined so that the Lagrangian for two non interacting compact objects reads $L_0 = \sum_a -m_a c^2 (1 - v_a^2/c^2)^{1/2}$. In other words, $m_a c^2$ represents the total energy of body a . This means that one has *implicitly* lumped in the definition of m_a many strong-self-gravity effects. [For instance, in tensor-scalar gravity m_a includes not only the usual Einsteinian gravitational binding energy due to the self-gravitational field $g_{\mu\nu}(x)$, but also the extra binding energy linked to the scalar field $\varphi(x)$.] Anyway, what is impor-

⁷In addition, scintillation data have led to an estimate of the sine of the orbital inclination, $\sin i$ (61). As said above, $\sin i$ numerically coincides with the PK parameter s measuring the ‘shape’ of the Shapiro time delay. Therefore, one could use the scintillation measurements as an indirect determination of s , thereby obtaining two independent tests from PSR J1141–6545 data. A caveat, however, is that the extraction of $\sin i$ from scintillation measurements rests on several simplifying assumptions whose validity is unclear. In fact, in the case of PSR J0737–3039 the direct timing measurement of s disagrees with its estimate via scintillation data (60). It is therefore safer not to use scintillation estimates of $\sin i$ on the same footing as direct timing measurements of the PK parameter s . On the other hand, a safe way of obtaining an s -related gravity test consists in using the necessary mathematical fact that $s = \sin i \leq 1$. In GR the definition $x_a = a_a \sin i/c$ leads to $\sin i = n x_a / (\beta_0 X_b)$. Therefore we can write the inequality $n x_a / (\beta_0(M) X_b) \leq 1$ as a phenomenological test of GR.

tant is that, when performing a phenomenological test from the measurement of a triplet of parameters, e.g. $\{k, \gamma, R\}$, at least one parameter among them be a priori sensitive to strong-field effects. This is enough for guaranteeing that the crossing of the three curves $k^{\text{theory}}(m_a, m_b) = k^{\text{obs}}$, $\gamma^{\text{theory}}(m_a, m_b) = \gamma^{\text{obs}}$, $R^{\text{theory}}(m_a, m_b) = R^{\text{obs}}$ is really a probe of strong-field gravity.

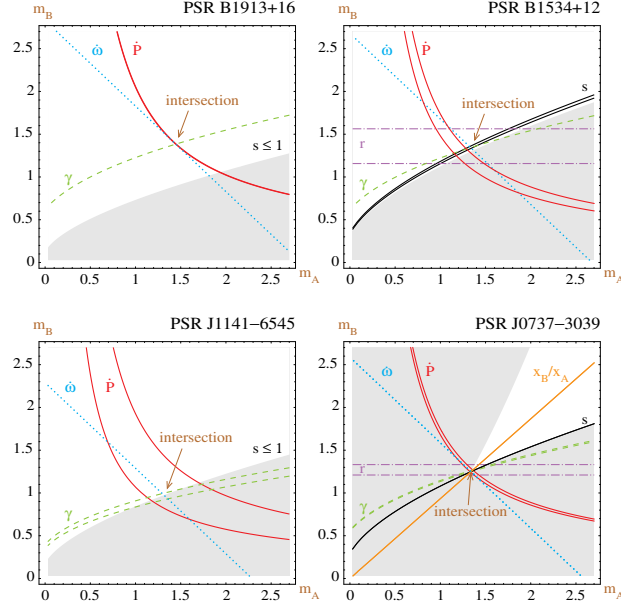


Figure A.1.: Phenomenological tests of General Relativity obtained from Keplerian and post-Keplerian timing parameters of four relativistic pulsars. Figure taken from (62).

In conclusion, the two recently discovered binary pulsars PSR J1141–6545 and PSR J0737–3039 have more than *doubled* the number of phenomenological tests of (radiative and) strong-field gravity. Before their discovery, the ‘canonical’ relativistic binary pulsars PSR 1913+16 and PSR 1534+12 had given us *four* such tests: one ($k - \gamma - \dot{P}_b$) test from PSR 1913+16 and three ($k - \gamma - r - s - \dot{P}_b$)⁸ tests from PSR 1534+12. The two new binary systems have given us *five*⁹ more phenomenological tests: one ($k - \gamma - \dot{P}_b$) (or two, $k - \gamma - \dot{P}_b - s$) tests from PSR J1141–6545 and four ($k - \gamma - r - s - \dot{P}_b - R$) tests from PSR J0737–3039¹⁰. As illustrated in Figure A.1, these *nine* phenomenological tests of strong-field (and radiative) gravity are all in beautiful

⁸The timing measurement of \dot{P}_b^{obs} in PSR 1534+12 is even more strongly affected by kinematic corrections (\dot{D} terms) than in the PSR 1913+16 case. In absence of a precise, independent measurement of the distance to PSR 1534+12, the $k - \gamma - \dot{P}_b$ test yields, at best, a $\sim 15\%$ test of GR.

⁹Or even six, if we use the scintillation determination of s in PSR J1141–6545.

¹⁰The companion pulsar 0737–3039B being non recycled, and being visible only during a small part of its orbit, cannot be timed with sufficient accuracy to allow one to measure any of its post-Keplerian parameters.

agreement with General Relativity.

In addition, let us recall that several quasi-circular wide binaries, made of a neutron star and a white dwarf, have led to high-precision phenomenological confirmations (53) (in strong-field conditions) of one of the deep predictions of General Relativity: the ‘strong’ equivalence principle, i.e. the fact that various bodies fall with the same acceleration in an external gravitational field, independently of the strength of their self-gravity.

Finally, let us mention that Ref. (41) has extended the philosophy of the phenomenological (parametrized post-Keplerian) analysis of timing data, to a similar phenomenological analysis of *pulse-structure data*. Ref. (41) showed that, in principle, one could extract up to 11 ‘post-Keplerian pulse-structure parameters’. Together with the 8 post-Keplerian timing parameters of a (single-line) binary pulsar, this makes a total of 19 phenomenological PK parameters. As these parameters depend not only on the two masses m_a, m_b but also on the two angles λ, η determining the direction of the spin axis of the pulsar, the maximum number of tests one might hope to extract from one (single-line) binary pulsar is $19 - 4 = 15$. However, the present accuracy with which one can model and measure the pulse structure of the known pulsars has not yet allowed one to measure any of these new pulse-structure parameters in a theory-independent and model-independent way.

Nonetheless, it has been possible to confirm the reality (and order of magnitude) of the spin-orbit coupling in GR which was pointed out (63; 64) to be observable via a secular change of the intensity profile of a pulsar signal. Confirmations of general relativistic spin-orbit effects in the evolution of pulsar profiles were obtained in several pulsars: PSR 1913+16 (65; 66), PSR B1534+12 (67) and PSR J1141–6545 (68). In this respect, let us mention that the spin-orbit interaction affects also several PK parameters, either by inducing a secular evolution in some of them (see (41)) or by contributing to their value. For instance, the spin-orbit interaction contributes to the observed value of the periastron advance parameter k an amount which is significant for the pulsars (such as 1913+16 and 0737–3039) where k is measured with high-accuracy. It was then pointed out (69) that this gives, in principle, an indirect way of measuring the moment of inertia of neutron stars (a useful quantity for probing the equation of state of nuclear matter (70; 71)). However, this can be done only if one measures, besides k , *two other* PK parameters with 10^{-5} accuracy. A rather tall order which will be a challenge to meet.

The phenomenological approach to pulsar tests has the advantage that it can confirm or invalidate a specific theory of gravity without making assumptions about other theories. Moreover, as General Relativity has no free parameters, any test of its predictions is a potentially lethal test. From this point of view, it is remarkable that GR has passed with flying colours all the pulsar tests it has been submitted to. [See, notably, Fig. A.1.] As argued above, these tests have probed strong-field aspects of gravity which had not

been probed by solar-system (or cosmological) tests. On the other hand, a disadvantage of the phenomenological tests is that they do not tell us in any precise way which strong-field structures, have been actually tested. For instance, let us imagine that one day one specific PPK test fails to be satisfied by GR, while the others are OK. This leaves us in a quandary: If we trust the problematic test, we must conclude that GR is wrong. However, the other tests say that GR is OK. This example shows that we would like to have some idea of what physical effects, linked to strong-field gravity, enter in each test, or even better in each PK parameter. The ‘effacement of internal structure’ which takes place in GR does not allow one to discuss this issue. This gives us a motivation for going beyond the phenomenological PPK approach by considering *theory-dependent* formalisms in which one embeds GR within a *space of alternative gravity theories*.

A.5. Theory-space approach to testing relativistic gravity with binary pulsar data

A complementary approach to testing gravity with binary pulsar data consists in embedding General Relativity within a *multi-parameter space of alternative theories of gravity*. In other words, we want to *contrast* the predictions of GR with the predictions of continuous families of alternative theories. In so doing we hope to learn more about which structures of GR are actually being probed in binary pulsar tests. This is a bit similar to the well-known psycho-physiological fact that the best way to appreciate a nuance of colour is to surround a given patch of colour by other patches with slightly different colours. This makes it much easier to detect subtle differences in colour. In the same way, we hope to learn about the probing power of pulsar tests by seeing how the phenomenological tests summarized in Fig. A.1 fail (or continue) to be satisfied when one continuously deform, away from GR, the gravity theory which is being tested.

Let us first recall the various ways in which this *theory-space approach* has been used in the context of the solar-system tests of relativistic gravity.

A.5.1. Theory-space approaches to solar-system tests of relativistic gravity

In the quasi-stationary weak-field context of the solar-system, this theory-space approach has been implemented in two different ways. First, the parametrized post-Newtonian (PPN) formalism (72; 73; 74; 51; 75; 76; 25; 77) describes many ‘directions’ in which generic alternative theories of gravity might differ in their *weak-field* predictions from GR. In its most general versions the

PPN formalism contains 10 ‘post-Einstein’ PPN parameters, $\bar{\gamma} \equiv \gamma^{\text{PPN}} - 1$ ¹¹, $\bar{\beta} \equiv \beta^{\text{PPN}} - 1$, ζ , $\alpha_1, \alpha_2, \alpha_3, \zeta_1, \zeta_2, \zeta_3, \zeta_4$. Each one of these dimensionless quantities parametrizes a certain class of slow-motion, weak-field gravitational effects which deviate from corresponding GR predictions. For instance, $\bar{\gamma}$ parametrizes modifications both of the effect of a massive body (say, the Sun) on the light passing near it, and of the terms in the two-body gravitational Lagrangian which are proportional to $(G m_a m_b / r_{ab}) \cdot (\mathbf{v}_a - \mathbf{v}_b)^2 / c^2$.

A second way of implementing the theory-space philosophy consists in considering some explicit, parameter-dependent family of alternative relativistic theories of gravity. For instance, the simplest tensor-scalar theory of gravity put forward by Jordan (78), Fierz (79) and Brans and Dicke (80) has a unique free parameter, say $\alpha_0^2 = (2\omega_{\text{BD}} + 3)^{-1}$. When $\alpha_0^2 \rightarrow 0$, this theory reduces to GR, so that α_0^2 (or $1/\omega_{\text{BD}}$) measures all the deviations from GR. When considering the weak-field limit of the Jordan-Fierz-Brans-Dicke (JFBD) theory, one finds that it can be described within the PPN formalism by choosing $\bar{\gamma} = -2\alpha_0^2(1 + \alpha_0^2)^{-1}$, $\bar{\beta} = 0$ and $\zeta = \alpha_i = \zeta_j = 0$.

Having briefly recalled the two types of theory-space approaches used to discuss solar-system tests, let us now consider the case of binary-pulsar tests.

A.5.2. Theory-space approaches to binary-pulsar tests of relativistic gravity

There exist generalizations of these two different theory-space approaches to the context of strong-field gravity and binary pulsar tests. First, the PPN formalism has been (partially) extended beyond the ‘first post-Newtonian’ (1PN) order deviations from GR ($\sim v^2/c^2 + Gm/c^2 r$) to describe 2PN order deviations from GR ($\sim \left(\frac{v^2}{c^2} + \frac{Gm}{c^2 r}\right)^2$) (81). Remarkably, there appear only two new parameters at the 2PN level¹²: ϵ and ζ . Also, by expanding in powers of the self-gravity parameters of body a and b the predictions for the PPK timing parameters in generic tensor-multi-scalar theories, one has shown that these predictions depended on several ‘layers’ of new dimensionless parameters (43). Early among these parameters one finds, the 1PN parameters $\bar{\beta}, \bar{\gamma}$ and then the basic 2PN parameters ϵ and ζ , but one also finds further parameters $\beta_3, (\beta\beta'), \beta'', \dots$ which would not enter usual 2PN effects. The two approaches that we have just mentioned can be viewed as generalizations

¹¹The PPN parameter γ^{PPN} is usually denoted simply as γ . To distinguish it from the Einstein-time-delay PPK timing parameter γ used above we add the superscript PPN. In addition, as the value of γ^{PPN} in GR is 1, we prefer to work with the parameter $\bar{\gamma} \equiv \gamma^{\text{PPN}} - 1$ which vanishes in GR, and therefore measures a ‘deviation’ from GR in a certain ‘direction’ in theory-space. Similarly with $\bar{\beta} \equiv \beta^{\text{PPN}} - 1$.

¹²When restricting oneself to the general class of tensor-multi-scalar theories. At the 1PN level, this restriction would imply that only the ‘directions’ $\bar{\gamma}$ and $\bar{\beta}$ are allowed.

of the PPN formalism.

There exist also useful generalizations to the strong-field context of the idea of considering some explicit parameter-dependent family of alternative theories of relativistic gravity. Early studies (21; 22; 48) focussed either on the one-parameter JFBD tensor-scalar theory, or on some theories which are not continuously connected to GR, such as Rosen's bimetric theory of gravity. Though the JFBD theory exhibits a marked difference from GR in that it predicts the existence of dipole radiation, it has the disadvantage that the weak field, solar-system constraints on its unique parameter α_0^2 are so strong that they drastically constrain (and essentially forbid) the presence of any non-radiative, strong-field deviations from GR. In view of this, it is useful to consider other 'mini-spaces' of alternative theories.

A two-parameter mini-space of theories, that we shall denote¹³ here as $T_2(\beta', \beta'')$, was introduced in (43). This two-parameter family of tensor-bi-scalar theories was constructed so as to have exactly the same first post-Newtonian limit as GR (i.e. $\bar{\gamma} = \bar{\beta} = \dots = 0$), but to differ from GR in its predictions for the various observables that can be extracted from binary pulsar data. Let us give one example of this behaviour of the $T_2(\beta', \beta'')$ class of theories. For a general theory of gravity we expect to have violations of the strong equivalence principle in the sense that the ratio between the gravitational mass of a self-gravitating body to its inertial mass will admit an expansion of the type

$$\frac{m_a^{\text{grav}}}{m_a^{\text{inert}}} \equiv 1 + \Delta_a = 1 - \frac{1}{2} \eta_1 c_a + \eta_2 c_a^2 + \dots \quad (\text{A.5.1})$$

where $c_a \equiv -2 \frac{\partial \ln m_a}{\partial \ln G}$ measures the 'gravitational compactness' (or fractional gravitational binding energy, $c_a \simeq -2 E_a^{\text{grav}} / m_a c^2$) of body a . The numerical coefficient η_1 of the contribution linear in c_a is a combination of the first post-Newtonian order PPN parameters, namely $\eta_1 = 4\bar{\beta} - \bar{\gamma}$ (51). The numerical coefficient η_2 of the term quadratic in c_a is a combination of the 1PN and 2PN parameters. When working in the context of the $T_2(\beta', \beta'')$ theories, the 1PN parameters vanish exactly ($\bar{\beta} = 0 = \bar{\gamma}$) and the coefficient of the quadratic term becomes simply proportional to the theory parameter β' : $\eta_2 = \frac{1}{2} B \beta'$, where $B \approx 1.026$. This example shows explicitly how binary pulsar data (here the data constraining the equivalence principle violation parameter $\Delta = \Delta_a - \Delta_b$, see above) can go beyond solar-system experiments in probing certain strong-self-gravity effects. Indeed, solar-system experiments are totally insensitive to 2PN parameters because of the smallness of $c_a \sim G m_a / c^2 R_a$ and of the structure of 2PN effects (81). By contrast, the 'compactness' of neutron stars is of order $c_a \sim 0.21 m_a / M_\odot \sim 0.3$ (43) so that the

¹³We add here an index 2 to T as a reminder that this is a class of tensor-*bi*-scalar theories, i.e. that they contain *two* independent scalar fields φ_1, φ_2 besides a dynamical metric $g_{\mu\nu}$.

pulsar limit $|\Delta| < 5.5 \times 10^{-3}$ (53) yields, within the $T_2(\beta', \beta'')$ framework, a significant limit on the dimensionless (2PN order) parameter β' : $|\beta'| < 0.12$.

Ref. (45) introduced a new two-parameter mini-space of gravity theories, denoted here as $T_1(\alpha_0, \beta_0)$, which, from the point of view of theoretical physics, has several advantages over the $T_2(\beta', \beta'')$ mini-space mentioned above. First, it is technically simpler in that it contains only *one* scalar field φ besides the metric $g_{\mu\nu}$ (hence the index 1 on $T_1(\alpha_0, \beta_0)$). Second, it contains only positive-energy excitations (while one combination of the two scalar fields of $T_2(\beta', \beta'')$ carried negative-energy waves). Third, it is the minimal way to parametrize the huge class of tensor-mono-scalar theories with a ‘coupling function’ $a(\varphi)$ satisfying some very general requirements (see below).

Let us now motivate the use of tensor-scalar theories of gravity as alternatives to general relativity.

A.5.3. Tensor-scalar theories of gravity

Let us start by recalling (essentially from (45)) why tensor-(mono)-scalar theories define a natural class of alternatives to GR. First, and foremost, the existence of scalar partners to the graviton is a simple theoretical possibility which has surfaced many times in the development of unified theories, from Kaluza-Klein to superstring theory. Second, they are general enough to describe many interesting deviations from GR (both in weak-field and in strong field conditions), but simple enough to allow one to work out their predictions in full detail.

Let us therefore consider a general tensor-scalar action involving a metric $\tilde{g}_{\mu\nu}$ (with signature ‘mostly plus’), a scalar field Φ , and some matter variables ψ_m (including gauge bosons):

$$S = \frac{c^4}{16\pi G_*} \int \frac{d^4x}{c} \tilde{g}^{1/2} [F(\Phi)\tilde{R} - Z(\Phi)\tilde{g}^{\mu\nu}\partial_\mu\Phi\partial_\nu\Phi - U(\Phi)] + S_m[\psi_m; \tilde{g}_{\mu\nu}]. \quad (\text{A.5.2})$$

For simplicity, we assume here that the weak equivalence principle is satisfied, i.e., that the matter variables ψ_m are all coupled to the same ‘physical metric’¹⁴ $\tilde{g}_{\mu\nu}$. The general model (A.5.2) involves three arbitrary functions: a function $F(\Phi)$ coupling the scalar Φ to the Ricci scalar of $\tilde{g}_{\mu\nu}$, $\tilde{R} \equiv R(\tilde{g}_{\mu\nu})$, a

¹⁴Actually, most unified models suggest that there are violations of the weak equivalence principle. However, the study of general string-inspired tensor-scalar models (82) has found that the composition-dependent effects would be negligible in the gravitational physics of neutron stars that we consider here. The experimental limits on tests of the equivalence principle would, however, bring a strong additional constraint of order $10^{-5} \alpha_0^2 \sim \Delta a/a \lesssim 10^{-12}$. As this constraint is strongly model-dependent, we will not use it in our exclusion plots below. One should, however, keep in mind that a limit on the scalar coupling strength α_0^2 of order $\alpha_0^2 \lesssim 10^{-7}$ (82; 83) is likely to exist in many, physically-motivated, tensor-scalar models.

function $Z(\Phi)$ renormalizing the kinetic term of Φ , and a potential function $U(\Phi)$. As we have the freedom of arbitrary redefinitions of the scalar field, $\Phi \rightarrow \Phi' = f(\Phi)$, only two functions among F , Z and U are independent. It is often convenient to rewrite (A.5.2) in a *canonical* form, obtained by redefining both Φ and $\tilde{g}_{\mu\nu}$ according to

$$g_{\mu\nu}^* = F(\Phi) \tilde{g}_{\mu\nu}, \quad (\text{A.5.3})$$

$$\varphi = \pm \int d\Phi \left[\frac{3}{4} \frac{F'^2(\Phi)}{F^2(\Phi)} + \frac{1}{2} \frac{Z(\Phi)}{F(\Phi)} \right]^{1/2}. \quad (\text{A.5.4})$$

This yields

$$S = \frac{c^4}{16\pi G_*} \int \frac{d^4x}{c} g_*^{1/2} [R_* - 2g_*^{\mu\nu} \partial_\mu \varphi \partial_\nu \varphi - V(\varphi)] + S_m [\psi_m; A^2(\varphi) g_{\mu\nu}^*], \quad (\text{A.5.5})$$

where $R_* \equiv R(g_{\mu\nu}^*)$, where the potential

$$V(\varphi) = F^{-2}(\Phi) U(\Phi), \quad (\text{A.5.6})$$

and where the *conformal coupling function* $A(\varphi)$ is given by

$$A(\varphi) = F^{-1/2}(\Phi), \quad (\text{A.5.7})$$

with $\Phi(\varphi)$ obtained by inverting the integral (A.5.4).

The two arbitrary functions entering the canonical form (A.5.5) are: (i) the conformal coupling function $A(\varphi)$, and (ii) the potential function $V(\varphi)$. Note that the ‘physical metric’ $\tilde{g}_{\mu\nu}$ (the one measured by laboratory clocks and rods) is conformally related to the ‘Einstein metric’ $g_{\mu\nu}^*$, being given by $\tilde{g}_{\mu\nu} = A^2(\varphi) g_{\mu\nu}^*$. The canonical representation is technically useful because it decouples the two irreducible propagating excitations: the spin-0 excitations are described by φ , while the pure spin-2 excitations are described by the *Einstein metric* $g_{\mu\nu}^*$ (with kinetic term the usual Einstein-Hilbert action $\propto R(g_{\mu\nu}^*)$).

In many technical developments it is useful to work with the *logarithmic coupling function* $a(\varphi)$ such that:

$$a(\varphi) \equiv \ln A(\varphi); \quad A(\varphi) \equiv e^{a(\varphi)}. \quad (\text{A.5.8})$$

In the case of the general model (A.5.2) this logarithmic¹⁵ coupling function is given by

$$a(\varphi) = -\frac{1}{2} \ln F(\Phi),$$

¹⁵As we shall mostly work with $a(\varphi)$ below, we shall henceforth drop the adjective ‘logarithmic’.

where $\Phi(\varphi)$ must be obtained from (A.5.4).

In the following, we shall assume that the potential $V(\varphi)$ is a slowly varying function of φ which, in the domain of variation we shall explore, is roughly equivalent to a very small mass term $V(\varphi) \sim 2m_\varphi^2(\varphi - \varphi_0)^2$ with m_φ^2 of cosmological order of magnitude $m_\varphi^2 = \mathcal{O}(H_0^2)$, or, at least, with a range $\lambda_\varphi = m_\varphi^{-1}$ much larger than the typical length scales that we shall consider (such as the size of the binary orbit, or the size of the Galaxy when considering violations of the strong equivalence principle). Under this assumption¹⁶ the potential function $V(\varphi)$ will only serve the role of fixing the value of φ far from the system (to $\varphi(r = \infty) = \varphi_0$), and its effect on the propagation of φ within the system will be negligible. In the end, the tensor-scalar phenomenology that we shall explore only depends on *one function*: the coupling function $a(\varphi)$.

Let us consider some examples to see what kind of coupling functions might naturally arise. First, the simplest case is the Jordan-Fierz-Brans-Dicke action, which is of the general type (A.5.2) with

$$F(\Phi) = \Phi \tag{A.5.9}$$

$$Z(\Phi) = \omega_{\text{BD}} \Phi^{-1}, \tag{A.5.10}$$

where ω_{BD} is an arbitrary constant. Using Eqs. (A.5.4), (A.5.7) above, one finds that $-2\alpha_0 \varphi = \ln \Phi$ and that the (logarithmic) coupling function is simply

$$a(\varphi) = \alpha_0 \varphi + \text{const.}, \tag{A.5.11}$$

where $\alpha_0 = \mp(2\omega_{\text{BD}} + 3)^{-1/2}$, depending on the sign chosen in Eq. (A.5.4). Independently of this sign, one has the link

$$\alpha_0^2 = \frac{1}{2\omega_{\text{BD}} + 3}. \tag{A.5.12}$$

Note that $2\omega_{\text{BD}} + 3$ must be positive for the spin-0 excitations to have the correct (non ghost) sign.

Let us now discuss the often considered case of a massive scalar field having a nonminimal coupling to curvature

$$S = \frac{c^4}{16\pi G_*} \int \frac{d^4x}{c} \tilde{g}^{1/2} \left(\tilde{R} - \tilde{g}^{\mu\nu} \partial_\mu \Phi \partial_\nu \Phi - m_\Phi^2 \Phi^2 + \zeta \tilde{R} \Phi^2 \right) + S_m[\psi_m; \tilde{g}_{\mu\nu}]. \tag{A.5.13}$$

¹⁶Note, however, that, as was recently explored in (84; 85; 86), a sufficiently fast varying potential $V(\varphi)$ can change the tensor-scalar phenomenology by endowing φ with a mass term $m_\varphi^2 = \frac{1}{4} \partial^2 V / \partial \varphi^2$ which strongly depends on the local value of φ and, thereby can get large in sufficiently dense environments.

This is of the form (A.5.2) with

$$F(\Phi) = 1 + \zeta\Phi^2, \quad Z(\Phi) = 1, \quad U(\Phi) = m_{\Phi}^2\Phi^2. \quad (\text{A.5.14})$$

The case $\zeta = -\frac{1}{6}$ is usually referred to as that of ‘conformal coupling’. With the variables (A.5.13) the theory is ghost-free only if $2(1 + \zeta\Phi^2)^2(d\varphi/d\Phi)^2 = 1 + \zeta(1 + 6\zeta)\Phi^2$ is everywhere positive. If we do not wish to restrict the initial values of Φ , we must have $\zeta(1 + 6\zeta) > 0$. Introducing then the notation $\chi \equiv \sqrt{\zeta(1 + 6\zeta)}$, we get the following link between Φ and φ :

$$2\sqrt{2}\varphi = \frac{\chi}{\zeta} \ln \left[1 + 2\chi\Phi \left(\sqrt{1 + \chi^2\Phi^2} + \chi\Phi \right) \right] + \sqrt{6} \ln \left[1 - 2\sqrt{6}\zeta\Phi \frac{\sqrt{1 + \chi^2\Phi^2} - \sqrt{6}\zeta\Phi}{1 + \zeta\Phi^2} \right]. \quad (\text{A.5.15})$$

For small values of Φ , this yields $\varphi = \Phi/\sqrt{2} + \mathcal{O}(\Phi^3)$. The potential and the coupling functions are given by

$$V(\varphi) = \frac{m_{\Phi}^2\Phi^2}{1 + \zeta\Phi^2}, \quad (\text{A.5.16})$$

$$a(\varphi) = -\frac{1}{2} \ln(1 + \zeta\Phi^2). \quad (\text{A.5.17})$$

These functions have singularities when $1 + \zeta\Phi^2$ vanishes. If we do not wish to restrict the initial value of Φ we must assume $\zeta > 0$ (which then implies our previous assumption $\zeta(1 + 6\zeta) > 0$). Then there is a one-to-one relation between Φ and φ over the entire real line. Small values of Φ correspond to small values of φ and to a coupling function

$$a(\varphi) = -\zeta\varphi^2 + \mathcal{O}(\varphi^4). \quad (\text{A.5.18})$$

On the other hand, large values of $|\Phi|$ correspond to large values of $|\varphi|$, and to a coupling function of the asymptotic form

$$a(\varphi) \simeq -\sqrt{2} \frac{\zeta}{\chi} |\varphi| + \text{const.} \quad (\text{A.5.19})$$

The potential $V(\varphi)$ has a minimum at $\varphi = 0$, as well as other minima at $\varphi \rightarrow \pm\infty$. If we assume, for instance, that m_{Φ}^2 and the cosmological dynamics are such that the cosmological value of φ is currently attracted towards zero, the value of φ at large distances from the local gravitating systems we shall consider will be $\varphi_0 \ll 1$.

As a final example of a possible tensor-scalar gravity theory, let us discuss the string-motivated dilaton-runaway scenario considered in (87). The start-

ing action (a functional of $\bar{g}_{\mu\nu}$ and Φ) was taken of the general form

$$S = \int d^4x \sqrt{\bar{g}} \left(\frac{B_g(\Phi)}{\alpha'} \bar{R} + \frac{B_\Phi(\Phi)}{\alpha'} [2\bar{\square}\Phi - (\bar{\nabla}\Phi)^2] - \frac{1}{4} B_F(\Phi) \bar{F}^2 - V(\Phi) + \dots \right),$$

and it was assumed that all the functions $B_i(\Phi)$ have a regular asymptotic behavior when $\Phi \rightarrow +\infty$ of the form $B_i(\Phi) = C_i + \mathcal{O}(e^{-\Phi})$. Under this assumption the early cosmological evolution can push Φ towards $+\infty$ (hence the name ‘runaway dilaton’). In the canonical, ‘Einstein frame’ representation (A.5.5), one has, for large values of Φ , $\Phi \simeq c\varphi$, where c is a numerical constant, and the coupling function to hadronic matter is given by

$$e^{a(\varphi)} \propto \Lambda_{\text{QCD}}(\varphi) \propto B_g^{-1/2}(\varphi) \exp[-8\pi^2 b_3^{-1} B_F(\varphi)]$$

where b_3 is the one-loop rational coefficient entering the renormalization-group running of the gauge field coupling g_F^2 . This finally yields a coupling function of the approximate form (for large values of φ):

$$a(\varphi) \simeq k e^{-c\varphi} + \text{const.},$$

where the dimensionless constants k and c are both expected to be of order unity. [The constant c must be positive, but the sign of k is not *a priori* restricted.]

Summarizing: the JFBD model yields a coupling function which is a linear function of φ , Eq. (A.5.11), a nonminimally coupled scalar yields a coupling function which interpolates between a quadratic function of φ , Eq. (A.5.18), and a linear one, Eq. (A.5.19), and the dilaton-runaway scenario of Ref. (87) yields a coupling function of a decaying exponential type.

A.5.4. The role of the coupling function $a(\varphi)$; definition of the two-dimensional space of tensor-scalar gravity theories $T_1(\alpha_0, \beta_0)$

Let us now discuss how the coupling function $a(\varphi)$ enters the observable predictions of tensor-scalar gravity at the first post-Newtonian (1PN) level, i.e., in the weak-field conditions appropriate to solar-system tests. It was shown in previous work that, if one uses appropriate units in the asymptotic region far from the system, namely units such that the asymptotic value $a(\varphi_0)$ of $a(\varphi)$ vanishes¹⁷, all observable quantities at the 1PN level depend only on the values of the first two derivatives of the $a(\varphi)$ at $\varphi = \varphi_0$. More precisely,

¹⁷In these units the Einstein metric $g_{\mu\nu}^*$ and the physical metric $\tilde{g}_{\mu\nu}$ asymptotically coincide.

if one defines

$$\alpha(\varphi) \equiv \frac{\partial a(\varphi)}{\partial \varphi}; \quad \beta(\varphi) \equiv \frac{\partial \alpha(\varphi)}{\partial \varphi} = \frac{\partial^2 a(\varphi)}{\partial \varphi^2}, \quad (\text{A.5.20})$$

and denotes by $\alpha_0 \equiv \alpha(\varphi_0)$, $\beta_0 \equiv \beta(\varphi_0)$ their asymptotic values, one finds (see, e.g., (43)) that the effective gravitational constant between two bodies (as measured by a Cavendish experiment) is given by

$$G = G_*(1 + \alpha_0^2), \quad (\text{A.5.21})$$

while, among the PPN parameters, only the two basic Eddington ones, $\bar{\gamma} \equiv \gamma^{\text{PPN}} - 1$, and $\bar{\beta} \equiv \beta^{\text{PPN}} - 1$, do not vanish, and are given by

$$\bar{\gamma} \equiv \gamma^{\text{PPN}} - 1 = -2 \frac{\alpha_0^2}{1 + \alpha_0^2}, \quad (\text{A.5.22})$$

$$\bar{\beta} \equiv \beta^{\text{PPN}} - 1 = \frac{1}{2} \frac{\alpha_0 \beta_0 \alpha_0}{(1 + \alpha_0^2)^2}. \quad (\text{A.5.23})$$

The structure of the results (A.5.22) and (A.5.23) can be transparently expressed by means of simple (Feynman-like) diagrams (see, e.g., (88)). Eqs. (A.5.21) and (A.5.22) correspond to diagrams where the interaction between two worldlines (representing two massive bodies) is mediated by the sum of the exchange of one graviton and one scalar particle. The scalar couples to matter with strength $\sim \alpha_0 \sqrt{G_*}$. The exchange of a scalar excitation then leads to a term $\propto \alpha_0^2$. On the other hand, Eq. (A.5.23) corresponds to a nonlinear interaction between three worldlines involving: (i) the ‘generation’ of a scalar excitation on a first worldline (factor α_0), (ii) a nonlinear vertex on a second worldline associated to the quadratic piece of $a(\varphi)$ ($a_{\text{quad}}(\varphi) = \frac{1}{2} \beta_0 (\varphi - \varphi_0)^2$); so that one gets a factor β_0), and (iii) the final ‘absorption’ of a scalar excitation on a third worldline (second factor α_0).

Eqs. (A.5.22) and (A.5.23) can be summarized by saying that the first two coefficients in the Taylor expansion of the coupling function $a(\varphi)$ around $\varphi = \varphi_0$ (after setting $a(\varphi_0) = 0$)

$$a(\varphi) = \alpha_0(\varphi - \varphi_0) + \frac{1}{2} \beta_0(\varphi - \varphi_0)^2 + \dots \quad (\text{A.5.24})$$

suffice to determine the quasi-stationary, weak-field (1PN) predictions of any tensor-scalar theory. In other words, the solar-system tests only explore the ‘osculating approximation’ (A.5.24) (slope and local curvature) to the function $a(\varphi)$. Note that GR corresponds to a vanishing coupling function $a(\varphi) = 0$ (so that $\alpha_0 = \beta_0 = \dots = 0$), the JFBD model corresponds to keeping only the first term on the R.H.S. of (A.5.24), while, for instance, the nonminimally coupled scalar field (with asymptotic value $\varphi_0 \ll 1$) does indeed lead to

nonzero values for both α_0 and β_0 , namely

$$\alpha_0 \simeq -2\zeta\varphi_0; \beta_0 \simeq -2\zeta. \quad (\text{A.5.25})$$

Finally the dilaton-runaway scenario considered above leads also to non zero values for both α_0 and β_0 , namely

$$\alpha_0 \simeq -kc e^{-c\varphi_0}; \beta_0 \simeq +kc^2 e^{-c\varphi_0}, \quad (\text{A.5.26})$$

for a largish value of φ_0 . Note that the dilaton-runaway model naturally predicts that $\alpha_0 \ll 1$, and that β_0 is of the same order of magnitude as α_0 : $\beta_0 \simeq -c\alpha_0$ with c being (positive and) of order unity. The interesting outcome is that such a model is well approximated by the usual JFBD model (with $\beta_0 = 0$). This shows that a JFBD-like theory could come out from a model which is initially quite different from the usual exact JFBD theory.

As we shall discuss in detail below, solar-system tests constrain α_0^2 and $\alpha_0^2|\beta_0|$ to be both small. This immediately implies that $|\alpha_0|$ must be small, i.e., that the scalar field is linearly weakly coupled to matter. On the other hand, the quadratic coupling parameter β_0 is not directly constrained. Both its magnitude and its sign can be more or less arbitrary. Note that there are no *a priori* sign restrictions on β_0 . The conformal factor $A^2(\varphi) = \exp(2a(\varphi))$ entering Eq. (A.5.5) had to be positive, but this leads to no restrictions on the sign of $a(\varphi)$ and of its various derivatives¹⁸. For instance, in the nonminimally coupled scalar field case, it seemed more natural to require $\zeta > 0$, which leads to a negative β_0 in view of Eq. (A.5.25).

Let us summarize the results above: (i) the most general tensor-scalar theory¹⁹ is described by one arbitrary function $a(\varphi)$; and (ii) weak-field tests depend only on the first two terms, parametrized by α_0 and β_0 , in the Taylor expansion (A.5.24) of $a(\varphi)$ around its asymptotic value φ_0 .

From this follows a rather natural way to define a simple *mini space of tensor-scalar theories*. It suffices to consider the two-dimensional space of theories, say $T_1(\alpha_0, \beta_0)$, defined by the coupling function which is a quadratic polynomial in φ (44; 45), say

$$a_{\alpha_0, \beta_0}(\varphi) = \alpha_0(\varphi - \varphi_0) + \frac{1}{2}\beta_0(\varphi - \varphi_0)^2. \quad (\text{A.5.27})$$

As indicated, this class of theories depends only on two parameters: α_0 and β_0 . The asymptotic value φ_0 of φ does not count as a third parameter (when

¹⁸As explained above, we assume here the presence of a potential term $V(\varphi)$ to fix the asymptotic value φ_0 of φ . If the potential $V(\varphi)$ is absent (or negligible), the ‘attractor mechanism’ of Refs. (89; 82) would attract φ to a *minimum* of the coupling function $a(\varphi)$, thereby favoring a *positive* value of β_0 .

¹⁹Under the assumption that the potential $V(\varphi)$ is a slowly-varying function of φ , which modifies the propagation of φ only on very large scales.

using the form (A.5.27)) because one can always work with the shifted field $\bar{\varphi} \equiv \varphi - \varphi_0$, with asymptotic value $\bar{\varphi}_0 = 0$ and coupling function $a_{\alpha_0, \beta_0}(\bar{\varphi}) = \alpha_0 \bar{\varphi} + \frac{1}{2} \beta_0 \bar{\varphi}^2$. Moreover, as already said, the asymptotic value $a(\varphi_0)$ of $a(\varphi)$ has also no physical meaning, because one can always use units such that it vanishes (as done in (A.5.27)).

Note also that an alternative way to represent the same class of theories is to use a coupling function of the very simple form

$$a_\beta(\varphi) = \frac{1}{2} \beta \varphi^2, \quad (\text{A.5.28})$$

but to keep the asymptotic value φ_0 as an independent parameter. This class of theories is clearly equivalent to $T_1(\alpha_0, \beta_0)$, Eq. (A.5.27), with the dictionary: $\alpha_0 = \beta \varphi_0$, $\beta_0 = \beta$.

A.5.5. Tensor-scalar gravity, strong-field effects, and binary-pulsar observables

Having chosen some mini-space of gravity theories, we now wish to derive what predictions these theories make for the timing observables of binary pulsars. To do this we need to generalize the general relativistic treatment of the motion and timing of binary systems comprising strongly self-gravitating bodies summarized above. Let us recall that this treatment was based on a multi-chart method, using a *matching* between two separate problems: (i) the ‘internal problem’ considers each strongly self-gravitating body in a suitable approximately freely falling frame where the influence of its companion is small, and (ii) the ‘external problem’ where the two bodies are described as effective point masses which interact via the various fields they are coupled to. Let us first consider the *internal problem*, i.e., the description of a neutron star in an approximately freely falling frame where the influence of the companion is reduced to imposing some boundary conditions on the tensor and scalar fields with which it interacts (21; 22; 43; 44; 45). The field equations of a general tensor-scalar theory, as derived from the canonical action (A.5.5) (neglecting the effect of $V(\varphi)$) read

$$R_{\mu\nu}^* = 2 \partial_\mu \varphi \partial_\nu \varphi + 8\pi G_* \left(T_{\mu\nu}^* - \frac{1}{2} T^* g_{\mu\nu}^* \right), \quad (\text{A.5.29})$$

$$\square_{g_*} \varphi = -4\pi G_* \alpha(\varphi) T_*, \quad (\text{A.5.30})$$

where $T_*^{\mu\nu} \equiv 2c (g_*)^{-1/2} \delta S_m / \delta g_{\mu\nu}^*$ denotes the material stress-energy tensor in ‘Einstein units’, and $\alpha(\varphi)$ the φ -derivative of the coupling function, see Eq. (A.5.20). All tensorial operations in Eqs. (A.5.29) and (A.5.30) are performed by using the Einstein metric $g_{\mu\nu}^*$.

Explicitly writing the field equations (A.5.29) and (A.5.30) for a slowly rotating (stationary, axisymmetric) neutron star, labelled²⁰ A , leads to a coupled set of ordinary differential equations constraining the radial dependence of $g_{\mu\nu}^*$ and φ (45; 90). Imposing the boundary conditions $g_{\mu\nu}^* \rightarrow \eta_{\mu\nu}$, $\varphi \rightarrow \varphi_a$ at large radial distances, finally determines the crucial ‘form factors’ (in Einstein units) describing the effective coupling between the neutron star A and the fields to which it is sensitive: total mass $m_A(\varphi_a)$, total scalar charge $\omega_A(\varphi_a)$, and inertia moment $I_A(\varphi_a)$. As indicated, these quantities are functions of the *asymptotic* value φ_a of φ felt by the considered neutron star²¹. They satisfy the relation $\omega_A(\varphi_a) = -\partial m_A(\varphi_a)/\partial \varphi_a$. From them, one defines other quantities that play an important role in binary pulsar physics, notably

$$\alpha_A(\varphi_a) \equiv -\frac{\omega_A}{m_A} \equiv \frac{\partial \ln m_A}{\partial \varphi_a}, \quad (\text{A.5.31})$$

$$\beta_A(\varphi_a) \equiv \frac{\partial \alpha_A}{\partial \varphi_a}, \quad (\text{A.5.32})$$

as well as

$$k_A(\varphi_a) \equiv -\frac{\partial \ln I_A}{\partial \varphi_a}. \quad (\text{A.5.33})$$

The quantity α_A , Eq. (A.5.31), plays a crucial role. It measures the *effective coupling strength* between the neutron star and the ambient scalar field. If we formally let the self-gravity of the neutron A tend toward zero (i.e., if we consider a weakly self-gravitating object), the function $\alpha_A(\varphi_a)$ becomes replaced by $\alpha(\varphi_a)$ where $\alpha(\varphi) \equiv \partial a(\varphi)/\partial \varphi$ is the coupling strength appearing in the R.H.S. of Eq. (A.5.30). Roughly speaking, we can think of $\alpha_A(\varphi_a)$ as a (suitable defined) average value of the local coupling strength $\alpha(\varphi(r))$ over the radial profile of the neutron star A .

It was pointed out in Refs. (44; 45) that the strong self-gravity of a neutron star can cause the effective coupling strength $\alpha_A(\varphi_a)$ to become of order unity, even when its weak-field counterpart $\alpha_0 = \alpha(\varphi_a)$ is extremely small (as is implied by solar-system tests that put strong constraints on the PPN combination $\bar{\gamma} = -2\alpha_0^2/(1 + \alpha_0^2)$). This is illustrated, in the minimal context

²⁰We henceforth use the labels A and B for the (recycled) pulsar and its companion, instead of the labels a and b used above. We henceforth use the label a to denote the *asymptotic* value of some quantity (at large radial distances within the local frame, X_A^i or X_B^i , of the considered neutron star A or B).

²¹This φ_a is a combination of the cosmological background value φ_0 and of the scalar influence of the companion of the considered neutron star. It varies with the orbital period and is determined as part of the ‘external problem’ discussed below. Note that, strictly speaking, the label a (for *asymptotic*) should be indexed by the label of the considered neutron star: i.e. one should use a label a_A (and a *locally asymptotic* value φ_{a_A}) when considering the neutron star A , and a label a_B (with a corresponding φ_{a_B}) when considering the neutron star B .

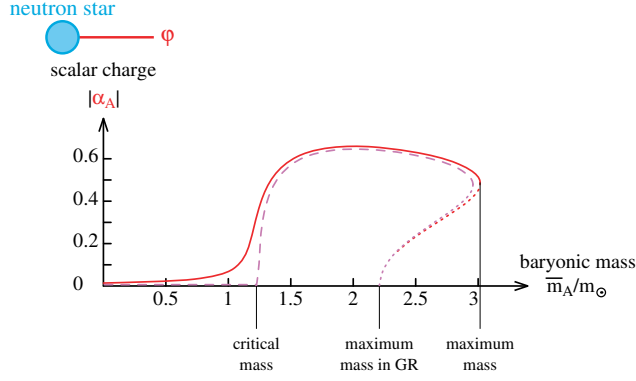


Figure A.2.: Dependence upon the baryonic mass \bar{m}_A of the coupling parameter α_A in the theory $T_1(\alpha_0, \beta_0)$ with $\alpha_0 = -0.014$, $\beta_0 = -6$. Figure taken from (91).

of the $T_1(\alpha_0, \beta_0)$ class of theories, in Figure A.2.

Note that when the baryonic mass \bar{m}_A of the neutron star is smaller than the critical mass $\bar{m}_{cr} \simeq 1.24 M_\odot$ the effective scalar coupling strength α_A of the star is quite small (because it is proportional to its weak-field limit $\alpha_0 = \alpha(\varphi_a)$). By contrast, when $\bar{m}_A > \bar{m}_{cr}$, $|\alpha_A|$ becomes of order unity, nearly independently of the externally imposed $\alpha_0 = \alpha_a = \alpha(\varphi_a)$. This interesting *non-perturbative* behaviour was related in (44; 45) to a mechanism of *spontaneous scalarization*, akin to the well-known mechanism of spontaneous magnetization of ferromagnets. See also (62) for a simple analytical description of the behaviour of α_A .

Let us also mention in passing that, in the case where A is a black hole, the effective coupling strength α_A actually *vanishes* (43). This result is related to the impossibility of having (regular) ‘scalar hair’ on a black hole.

We have sketched above the first part of the matching approach to the motion and timing of strongly self-gravitating bodies: the ‘internal problem’. It remains to describe the remaining ‘external problem’. As already mentioned (and emphasized, in the present context, by Eardley (21; 25)), the most efficient way to describe the external problem is, instead of matching in detail the external fields $(g_{\mu\nu}^*, \varphi)$ to the fields generated by each body in its comoving frame, to ‘skeletonize’ the bodies by point masses. Technically this means working with the effective action

$$\begin{aligned}
S &= \frac{c^4}{16\pi G_*} \int \frac{d^D x}{c} g_*^{1/2} [R_* - 2 g_*^{\mu\nu} \partial_\mu \varphi \partial_\nu \varphi] \\
&\quad - \sum_A c \int m_A(\varphi(z_A)) (-g_{\mu\nu}^*(z_A) dz_A^\mu dz_A^\nu)^{1/2}, \quad (\text{A.5.34})
\end{aligned}$$

where the function $m_A(\varphi)$ in the last term on the R.H.S. is the function $m_A(\varphi_a)$

obtained above by solving the internal problem. Eq. (A.5.34) indicates that the argument of this function is taken to be $\varphi_a = \varphi(z_A)$, i.e., the value that the scalar field (as viewed in the external problem) takes at the location z_A^μ of the center of mass of body A . However, as body A is described, in the external problem, as a point mass this causes a technical difficulty: the externally determined field $\varphi(x)$ becomes formally singular at the location of the point sources, so that $\varphi(z_A)$ is *a priori* undefined. One can either deal with this problem by coming back to the physically well-defined matching approach (which shows that $\varphi(z_A)$ should be replaced by φ_a , the value of φ in an intermediate domain $R_A \ll r \ll |z_A - z_B|$), or use the efficient technique of dimensional regularization. This means that the spacetime dimension D in Eq. (A.5.34) is first taken to have a complex value such that $\varphi(z_A)$ is finite, before being analytically continued to its physical value $D = 4$.

One then derives from the action (A.5.34) two important consequences for the motion and timing of binary pulsars. First, one derives the Lagrangian describing the relativistic interaction between N strongly self-gravitating bodies (including orbital $\sim (v/c)^2$ effects, and neglecting $\mathcal{O}(v^4/c^4)$ ones) (25; 21; 43; 48). It is the sum of one-body, two-body and three-body terms.

The one-body action has the usual form of the sum (over the label A) of the kinetic term of each point mass:

$$\begin{aligned} L_A^{\text{one-body}} &= -m_A c^2 \sqrt{1 - \mathbf{v}_A^2/c^2} \\ &= -m_A c^2 + \frac{1}{2} m_A \mathbf{v}_A^2 + \frac{1}{8} m_A \frac{(\mathbf{v}_A^2)^2}{c^2} + \mathcal{O}\left(\frac{1}{c^4}\right). \end{aligned} \quad (\text{A.5.35})$$

Here, we use Einstein units, and the inertial mass m_A entering Eq. (A.5.35) is $m_A \equiv m_A(\varphi_0)$, where φ_0 is the asymptotic value of φ far away from the considered N -body system.

The two-body action is a sum over the pairs A, B of a term $L_{AB}^{2\text{-body}}$ which differs from the GR-predicted 2-body Lagrangian in two ways: (i) the usual gravitational constant G appearing as an overall factor in $L_{AB}^{2\text{-body}}$ must be replaced by an effective (body-dependent) gravitational constant (in the appropriate units mentioned above) given by

$$G_{AB} = G_*(1 + \alpha_A \alpha_B), \quad (\text{A.5.36})$$

and (ii) the relativistic ($\mathcal{O}(v^2/c^2)$) terms in $L_{AB}^{2\text{-body}}$ contain, in addition to those predicted by GR, new velocity-dependent terms of the form

$$\delta^\gamma L_{AB}^{2\text{-body}} = (\bar{\gamma}_{AB}) \frac{G_{AB} m_A m_B}{r_{AB}} \frac{(\mathbf{v}_A - \mathbf{v}_B)^2}{c^2}, \quad (\text{A.5.37})$$

with

$$\tilde{\gamma}_{AB} \equiv \gamma_{AB} - 1 = -2 \frac{\alpha_A \alpha_B}{1 + \alpha_A \alpha_B}. \quad (\text{A.5.38})$$

In these expressions $\alpha_A \equiv \alpha_A(\varphi_0) \equiv \partial \ln m_A(\varphi_0) / \partial \varphi_0$ (see Eq. (A.5.31) with $\varphi_a \rightarrow \varphi_0$).

Finally, the 3-body action is a sum over the pairs B, C and over A (with $A \neq B, A \neq C$, but the possibility of having $B = C$) of

$$L_{ABC}^{3\text{-body}} = -(1 + 2\tilde{\beta}_{BC}^A) \frac{G_{AB} G_{AC} m_A m_B m_C}{c^2 r_{AB} r_{AC}} \quad (\text{A.5.39})$$

where

$$\tilde{\beta}_{BC}^A \equiv \beta_{BC}^A - 1 = \frac{1}{2} \frac{\alpha_B \beta_A \alpha_C}{(1 + \alpha_A \alpha_B)(1 + \alpha_A \alpha_C)}, \quad (\text{A.5.40})$$

with $\beta_A = \partial \alpha_A(\varphi_0) / \partial \varphi_0$ (see Eq. (A.5.32) with $\varphi_a \rightarrow \varphi_0$).

When comparing the strong-field results (A.5.36), (A.5.38), (A.5.40) to their weak-field counterparts (A.5.21), (A.5.22), (A.5.23) one sees that the body-dependent quantity α_A replaces the weak-field coupling strength α_0 in all quantities which are linked to a scalar effect generated by body A . Note also that, in keeping with the ‘3-body’ nature of Eq. (A.5.39), the quantity $\beta_{BC}^A - 1$ is linked to scalar interactions which are generated in bodies B and C and which nonlinearly interact on body A . The notation used above has been chosen to emphasize that γ_{AB} and β_{BC}^A are strong-field analogs of the usual Eddington parameters $\gamma^{\text{PPN}}, \beta^{\text{PPN}}$, so that $\tilde{\gamma}_{AB}$ and $\tilde{\beta}_{BC}^A$ are strong-field analogs of the ‘post-Einstein’ 1PN parameters $\tilde{\gamma}$ and $\tilde{\beta}$ (which vanish in GR). Indeed the usual PPN results for the post-Einstein terms in the $\mathcal{O}(1/c^2)$ 2-body and 3-body Lagrangians are obtained by replacing in Eqs. (A.5.37) and (A.5.39) $\tilde{\gamma}_{AB} \rightarrow \tilde{\gamma}$, $\tilde{\beta}_{BC}^A \rightarrow \tilde{\beta}$ and $G_{AB} \rightarrow G$.

The non-perturbative strong-field effects discussed above show that the strong self-gravity of neutron stars can cause γ_{AB} and β_{BC}^A to be significantly different from their GR values $\gamma^{\text{GR}} = 1, \beta^{\text{GR}} = 1$, in some scalar-tensor theories having a small value of the basic coupling parameter α_0 (so that $\gamma^{\text{PPN}} - 1 \propto \alpha_0^2$ and $\beta^{\text{PPN}} - 1 \propto \beta_0 \alpha_0^2$ are both small). For instance, Fig. A.2 shows that it is possible to have $\alpha_A \sim \alpha_B \sim \pm 0.6$ which implies $\gamma_{AB} - 1 \sim -0.53$, i.e., a 50% deviation from GR! Even larger effects can arise in $\beta_{BC}^A - 1$ because of the large values that $\beta_A = \partial \alpha_A / \partial \varphi_0$ can reach near the spontaneous scalarization transition (45).

Those possible strong-field modifications of the effective Eddington parameters $\gamma_{AB}, \beta_{BC}^A$, which parametrize the ‘first post-Keplerian’ (1PK) effects (i.e., the orbital effects $\sim v^2/c^2$ smaller than those entailed by the Lagrangian $\sum_A \frac{1}{2} m_A v_A^2 + \frac{1}{2} \sum_{A \neq B} G_{AB} m_A m_B / r_{AB}$), can then significantly modify the usual GR predictions relating the directly observable parametrized post-Keplerian

(PPK) parameters to the values of the masses of the pulsar and its companion. As worked out in Refs. (25; 41; 43; 45) one finds the following modified predictions for the PPK parameters $k \equiv \langle \dot{\omega} \rangle / n$, r and s :

$$k^{\text{th}}(m_A, m_B) = \frac{3}{1 - e^2} \left(\frac{G_{AB}(m_A + m_B) n}{c^3} \right)^{2/3} \left[\frac{1 - \frac{1}{3} \alpha_A \alpha_B}{1 + \alpha_A \alpha_B} - \frac{X_A \beta_B \alpha_A^2 + X_B \beta_A \alpha_B^2}{6(1 + \alpha_A \alpha_B)^2} \right], \quad (\text{A.5.41})$$

$$r^{\text{th}}(m_A, m_B) = G_{0B} m_B, \quad (\text{A.5.42})$$

$$s^{\text{th}}(m_A, m_B) = \frac{n x_A}{X_B} \left[\frac{G_{AB}(m_A + m_B) n}{c^3} \right]^{-1/3}. \quad (\text{A.5.43})$$

Here, the label A refers to the object which is timed ('the pulsar'²²), the label B refers to its companion, $x_A = a_A \sin i / c$ denotes the projected semi-major axis of the orbit of A (in light seconds), $X_A \equiv m_A / (m_A + m_B)$ and $X_B \equiv m_B / (m_A + m_B) = 1 - X_A$ the mass ratios, $n \equiv 2\pi / P_b$ the orbital frequency and $G_{0B} = G_*(1 + \alpha_0 \alpha_B)$ the effective gravitational constant measuring the interaction between B and a test object (namely electromagnetic waves on their way from the pulsar toward the Earth). In addition one must replace the unknown bare Newtonian G_* by its expression in terms of the one measured in Cavendish experiments, i.e., $G_* = G / (1 + \alpha_0^2)$ as deduced from Eq. (A.5.21).

The modified theoretical prediction for the PPK parameter γ entering the 'Einstein time delay' Δ_E , Eq. (A.3.16), is more complicated to derive because one must take into account the modulation of the proper spin period of the pulsar caused by the variation of its moment of inertia I_A under the (scalar) influence of its companion (25; 21; 45). This leads to

$$\gamma^{\text{th}}(m_A, m_B) = \frac{e}{n} \frac{X_B}{1 + \alpha_A \alpha_B} \left(\frac{G_{AB}(m_A + m_B) n}{c^3} \right)^{2/3} [X_B(1 + \alpha_A \alpha_B) + 1 + k_A \alpha_B], \quad (\text{A.5.44})$$

where $k_A(\varphi_0) = -\partial \ln I_A(\varphi_0) / \partial \varphi_0$ (see Eq. (A.5.33) with $\varphi_a \rightarrow \varphi_0$). Numerical studies (45) show that k_A can take quite large values. Actually, the quantity $k_A \alpha_B$ entering (A.5.44) blows up near the scalarization transition when $\alpha_0 \rightarrow 0$ (keeping $\beta_0 < 0$ fixed). In other words a theory which is closer to GR in weak-field conditions predicts larger deviations in the strong-field regime.

The structure dependence of the effective gravitational constant G_{AB} , Eq. (A.5.36),

²²In the double binary pulsar, both the first discovered pulsar and its companion are pulsars. However, the companion B is a non recycled, slow pulsar whose motion is well described by Keplerian parameters only.

has also the consequence that the object A does not fall in the same way as B in the gravitational field of the Galaxy. As most of the mass of the Galaxy is made of non strongly-self-gravitating bodies, A will fall toward the Galaxy with an acceleration $\propto G_{A0}$, while B will fall with an acceleration $\propto G_{B0}$. Here, as above, $G_{A0} = G_{0A} = G_*(1 + \alpha_0 \alpha_A)$ is the effective gravitational constant between A and any weakly self-gravitating body. As pointed out in Ref. (52) this possible violation of the universality of free fall of self-gravitating bodies can be constrained by using observational data on the class of small-eccentricity long-orbital-period binary pulsars. More precisely, the quantity which can be observationally constrained is not exactly the violation $\Delta_{AB} = (G_{0A} - G_{0B})/G = (1 + \alpha_0^2)^{-1}(\alpha_0 \alpha_A - \alpha_0 \alpha_B)$ of the strong equivalence principle [which simplifies to $\Delta_{A0} = (G_{0A} - G)/G = (1 + \alpha_0^2)^{-1}(\alpha_0 \alpha_A - \alpha_0^2)$ in the case of observational relevance where one neglects the self-gravity of the white-dwarf companion] but rather²³ (43)

$$\Delta^{\text{effective}} \equiv \left(\frac{2\gamma_{AB} - (X_A \beta_{AA}^B + X_B \beta_{BB}^A) + 2}{3} \right)^{-1} (1 + \alpha_A \alpha_B)^{-3/2} (1 + \alpha_0^2)^{-1} (\alpha_0 \alpha_A - \alpha_0 \alpha_B). \quad (\text{A.5.45})$$

Here, the index B (= white-dwarf companion) can be replaced by 0 (weakly self-gravitating body) so that, for instance, $\gamma_{AB} = \gamma_{A0} = 1 - 2\alpha_A \alpha_0 / (1 + \alpha_A \alpha_0) = (1 - \alpha_A \alpha_0) / (1 + \alpha_A \alpha_0)$, as deduced from Eq. (A.5.38).

It remains to discuss the possible strong-field modifications of the theoretical prediction for the orbital period derivative $\dot{P}_b = \dot{P}_b^{\text{th}}(m_A, m_B)$. This is obtained by deriving from the effective action (A.5.34) the energy lost by the binary system in the form of fluxes of spin-2 and spin-0 waves at infinity. The needed results in a generic tensor-scalar theory were derived in Refs. (43; 48) (in addition one must take into account the tensor-scalar modification of the additional ‘varying-Doppler’ contribution to the observed \dot{P}_b due to the Galactic acceleration (47)). The final result for \dot{P}_b is of the form

$$\begin{aligned} \dot{P}_b^{\text{th}}(m_A, m_B) &= \dot{P}_{b\varphi}^{\text{monopole}} + \dot{P}_{b\varphi}^{\text{dipole}} + \dot{P}_{b\varphi}^{\text{quadrupole}} + \dot{P}_{bg^*}^{\text{quadrupole}} \\ &+ \dot{P}_{b\text{GR}}^{\text{galactic}} + \delta^{\text{th}} \dot{P}_b^{\text{galactic}}, \end{aligned} \quad (\text{A.5.46})$$

where, for instance, $\dot{P}_{b\varphi}^{\text{monopole}}$ is (heuristically²⁴) related to the monopolar flux

²³This refinement is given here for pedagogical completeness. However, in practice, the lowest-order result $\Delta \simeq (1 + \alpha_0^2)^{-1}(\alpha_0 \alpha_A - \alpha_0^2) \simeq \alpha_0 \alpha_A - \alpha_0^2$ is accurate enough.

²⁴Contrary to the GR case where a lot of effort was spent to show how the observed \dot{P}_b was directly related to the GR predictions for the $(v/c)^5$ -accurate orbital equations of motion of a binary system (23), we use here the indirect and less rigorous argument that the energy flux at infinity should be balanced by a corresponding decrease of the mechanical energy of the binary system.

of spin-0 waves at infinity. The term $\dot{P}_{bg^*}^{\text{quadrupole}}$ corresponds to the usual quadrupolar flux of spin-2 waves at infinity. It reads:

$$\dot{P}_{bg^*}^{\text{quadrupole}}(m_A, m_B) = -\frac{192\pi}{5(1 + \alpha_A \alpha_B)} \frac{m_A m_B}{(m_A + m_B)^2} \left(\frac{G_{AB}(m_A + m_B) n}{c^3} \right)^{5/3} \frac{1 + 73 e^2/24 + 37 e^4/96}{(1 - e^2)^{7/2}}, \quad (\text{A.5.47})$$

with $G_{AB} = G_*(1 + \alpha_A \alpha_B) = G(1 + \alpha_A \alpha_B)/(1 + \alpha_0^2)$, where G_* is the ‘bare’ gravitational constant appearing in the action, while G is the gravitational constant measured in Cavendish experiments. The flux (A.5.47) is the only one which survives in GR (although without any α_A -related modifications). Among the several other contributions which arise in tensor-scalar theories, let us only write down the explicit expression of the contribution to (A.5.46) coming from the *dipolar flux of scalar waves*. Indeed, this contribution is, in most cases, the dominant one (21) because it scales as $(v/c)^3$, while the monopolar and quadrupolar contributions scale as $(v/c)^5$. It reads

$$\dot{P}_{b\phi}^{\text{dipole}}(m_A, m_B) = -2\pi \frac{G_* m_A m_B n}{c^3(m_A + m_B)} \frac{1 + e^2/2}{(1 - e^2)^{5/2}} (\alpha_A - \alpha_B)^2. \quad (\text{A.5.48})$$

Note that the dipolar effect (A.5.48) vanishes when $\alpha_A = \alpha_B$. Indeed, a binary system made of two identical objects ($A = B$) cannot select a preferred direction for a dipole vector, and cannot therefore emit any dipolar radiation. This also implies that double neutron star systems (which tend to have $m_A \approx m_B \sim 1.35 M_\odot$) will be rather poor emitters of dipolar radiation (though (A.5.48) still tends to dominate over the other terms in (A.5.46), because of the remaining difference $(m_A - m_B)/(m_A + m_B) \neq 0$). By contrast, very dissymmetric systems such as a neutron-star and a white-dwarf (or a neutron-star and a black hole) will be very efficient emitters of dipolar radiation, and will potentially lead to very strong constraints on tensor-scalar theories. See below.

A.5.6. Theory-space analyses of binary pulsar data

Having reviewed the theoretical results needed to discuss the predictions of alternative gravity theories, let us end by summarizing the results of various theory-space analyses of binary pulsar data.

Let us first recall what are the best, current solar-system limits on the two 1PN ‘post-Einstein’ parameters $\bar{\gamma} \equiv \gamma^{\text{PPN}} - 1$ and $\bar{\beta} \equiv \beta^{\text{PPN}} - 1$. They are:

$$\bar{\gamma} = (2.1 \pm 2.3) \times 10^{-5}, \quad (\text{A.5.49})$$

from frequency shift measurements made with the Cassini spacecraft (92),

which supersedes the constraint

$$\bar{\gamma} = (-1.7 \pm 4.5) \times 10^{-4} \quad (\text{A.5.50})$$

from VLBI measurements (93),

$$|2\bar{\gamma} - \bar{\beta}| < 3 \times 10^{-3}, \quad (\text{A.5.51})$$

from Mercury's perihelion shift (77; 94), and

$$4\bar{\beta} - \bar{\gamma} = (4.4 \pm 4.5) \times 10^{-4}, \quad (\text{A.5.52})$$

from Lunar laser ranging measurements (95).

Concerning binary pulsar data, we can make use of the published measurements of various Keplerian and post-Keplerian timing parameters in the binary pulsars: PSR 1913+16 (46), PSR B1534+12 (50), PSR J1141–6545 (56) and PSR J0737–3039A+B (58; 59; 60). In addition, we can use²⁵ the recently updated limit on the parameter Δ measuring a possible violation of the strong equivalence principle (SEP), namely $|\Delta| < 5.5 \times 10^{-3}$ at the 95% confidence level (53).

This ensemble of solar-system and binary-pulsar data can then be analyzed within any given parametrized theoretical framework. For instance, one might work within

- (i) the 4-parameter framework $T_0(\bar{\gamma}, \bar{\beta}; \epsilon, \zeta)$ (81) which defines the 2PN extension of the original (Eddington) PPN framework $T_0(\bar{\gamma}, \bar{\beta})$; or
- (ii) the 2-parameter class of tensor-mono-scalar theories $T_1(\alpha_0, \beta_0)$ (44); or
- (iii) the 2-parameter class of tensor-bi-scalar theories $T_2(\beta', \beta'')$ (43).

Here, the index 0 on $T_0(\bar{\gamma}, \bar{\beta}; \epsilon, \zeta)$ is a reminder of the fact that this framework is not a family of specific theories (it contains *zero* explicit dynamical fields), but is a parametrization of 2PN deviations from GR. As a consequence, its use for analyzing binary pulsar data is somewhat ill-defined because one needs to truncate the various timing observables (which are functions of the compactness of the two bodies A and B , say $P^{\text{PK}} = f(c_A, c_B)$) at the 2PN order (i.e. essentially at the quadratic order in c_A and/or c_B). For some observables (or for product of observables) there might be several ways of defining this truncation. In spite of this slight inconvenience, the use of the $T_0(\bar{\gamma}, \bar{\beta}; \epsilon, \zeta)$ framework is conceptually useful because it shows very clearly

²⁵There is, however, a caveat in the theoretical use one can make of the phenomenological limits on Δ . Indeed, in the small-eccentricity long-orbital-period binary pulsar systems used to constrain Δ one does not have access to enough PK parameters to measure the pulsar mass m_A directly. As the theoretical expression of $\Delta \simeq \alpha_0 \alpha_A - \alpha_0^2$ depends on m_A (through α_A), one needs to assume some fiducial value of m_A (say $m_A \simeq 1.35 M_\odot$).

why and how binary-pulsar data can probe the behaviour of gravitational theories beyond the usual 1PN regime probed by solar-system tests.

For instance, the parameter $\Delta_A \equiv m_A^{\text{grav}}/m_A^{\text{inert}} - 1$ measuring the strong equivalence principle (SEP) violation in a neutron star has, within the $T_0(\bar{\gamma}, \bar{\beta}; \epsilon, \zeta)$ framework, a 2PN-order expansion of the form (43; 81)

$$\Delta_A = -\frac{1}{2} (4\bar{\beta} - \bar{\gamma}) c_A + \left(\frac{\epsilon}{2} + \zeta + \mathcal{O}(\bar{\beta}) \right) b_A, \quad (\text{A.5.53})$$

where $c_A = -2 \frac{\partial \ln m_A}{\partial \ln G} \simeq \frac{1}{c^2} \langle U \rangle_A$, $b_A = \frac{1}{c^4} \langle U^2 \rangle_A \simeq B c_A^2$, with $B \simeq 1.026$ and $c_A \simeq k m_A / M_\odot$ with $k \sim 0.21$. The general result (A.5.53) is compatible with the result quoted in subsection A.5.2 within the context of the theory $T_2(\beta', \beta'')$ when taking into account the fact that, within $T_2(\beta', \beta'')$, one has $\bar{\beta} = \bar{\gamma} = 0$, $\epsilon = \beta'$ and $\zeta = 0$ [and that β'' parametrizes some effects beyond the 2PN level].

On the example of Eq. (A.5.53) one sees that, after having used solar-system tests to constrain the first contribution on the RHS to a very small value, one can use binary-pulsar tests of the SEP to set a significant limit on the combination $\frac{1}{2} \epsilon + \zeta$ of 2PN parameters. Other pulsar data then yield significant limits on other combinations of the two 2PN parameters ϵ and ζ . The final conclusion is that binary-pulsar data allow one to set significant limits (around or better than the 1% level) on the possible 2PN deviations from GR (in contrast to solar-system tests which are unable to yield any limit on ϵ and ζ) (81). For a recent update of the limits on ϵ and ζ , which makes use of recent pulsar data see (62).

Let us now briefly discuss the use of mini-space of theories, such as $T_1(\alpha_0, \beta_0)$ or $T_2(\beta', \beta'')$, for analyzing solar-system and binary-pulsar data. The basic methodology is to compute, for each given theory (e.g. for each given values of α_0 and β_0 if one chooses to work in the $T_1(\alpha_0, \beta_0)$ theory space) a goodness-of-fit statistics $\chi^2(\alpha_0, \beta_0)$ measuring the quality of the agreement between the experimental data and the considered theory. For instance, when considering the timing data of a particular pulsar, for which one has measured several PK parameters p_i ($i = 1, \dots, n$) with some standard deviations $\sigma_{p_i}^{\text{obs}}$, one defines, for this pulsar

$$\chi^2(\alpha_0, \beta_0) = \min_{m_A, m_B} \sum_{i=1}^n (\sigma_{p_i}^{\text{obs}})^{-2} (p_i^{\text{theory}}(\alpha_0, \beta_0; m_A, m_B) - p_i^{\text{obs}})^2, \quad (\text{A.5.54})$$

where ‘min’ denotes the result of minimizing over the unknown masses m_A, m_B and where $p_i^{\text{theory}}(\alpha_0, \beta_0; m_A, m_B)$ denotes the theoretical prediction (within $T_1(\alpha_0, \beta_0)$) for the PK observable p_i (given also the observed values of the Keplerian parameters).

The goodness-of-fit quantity $\chi^2(\alpha_0, \beta_0)$ will reach its minimum χ_{min}^2 for

some values, say $\alpha_0^{\min}, \beta_0^{\min}$, of α_0 and β_0 . Then, one focusses, for each pulsar, on the level contours of the function

$$\Delta \chi^2(\alpha_0, \beta_0) \equiv \chi^2(\alpha_0, \beta_0) - \chi_{\min}^2. \quad (\text{A.5.55})$$

Each choice of level contour (e.g. $\Delta \chi^2 = 1$ or $\Delta \chi^2 = 2.3$) defines a certain region in theory space, which contains, with a certain corresponding ‘confidence level’, the ‘correct’ theory of gravity (if it belongs to the considered mini-space of theories). When combining together several independent data sets (e.g. solar-system data, and different pulsar data) we can define a total goodness-of-fit statistics $\chi_{\text{tot}}^2(\alpha_0, \beta_0)$, by adding together the various individual $\chi^2(\alpha_0, \beta_0)$. This leads to a corresponding combined contour $\Delta \chi_{\text{tot}}^2(\alpha_0, \beta_0)$.

Let us end by briefly summarizing the results of the theory-space approach to relativistic gravity tests. For detailed discussions the reader should consult Refs. (43; 49; 45; 29; 91), and especially the recent update (62) which uses the latest binary-pulsar data.

Regarding the two-parameter class of tensor-bi-scalar theories $T_2(\beta', \beta'')$ the recent analysis (62) has shown that the $\Delta \chi^2(\beta', \beta'')$ corresponding to the double binary pulsar PSR J0737–3039 was defining quite a small elliptical allowed region in the (β', β'') plane. By contrast the other pulsar data define much wider allowed regions, while the strong equivalence principle tests define (in view of the theoretical result $\Delta \simeq 1 + \frac{1}{2} B \beta' (c_A^2 - c_B^2)$) a thin, but infinitely long, strip $|\beta'| < \text{cst.}$ in the (β', β'') plane. This highlights the power of the double binary pulsar in probing certain specific strong-field deviations from GR.

Contrary to the $T_2(\beta', \beta'')$ tensor-bi-scalar theories, which were constructed to have exactly the same first post-Newtonian limit as GR²⁶ (so that solar-system tests put no constraints on β' and β''), the class of tensor-mono-scalar theories $T_1(\alpha_0, \beta_0)$ is such that its parameters α_0 and β_0 parametrize *both* the weak-field 1PN regime (see Eqs. (A.5.22) and (A.5.23) above) and the strong-field regime (which plays an important role in compact binaries). This means that each class of solar-system data (see Eqs. (A.5.49)–(A.5.52) above) will define, via a corresponding goodness-of-fit statistics of the type, say

$$\chi_{\text{Cassini}}^2(\alpha_0, \beta_0) = (\sigma_{\gamma}^{\text{Cassini}})^{-2} (\bar{\gamma}^{\text{theory}}(\alpha_0, \beta_0) - \bar{\gamma}^{\text{Cassini}})^2$$

a certain allowed region²⁷ in the (α_0, β_0) plane. As a consequence, the anal-

²⁶However, this could be achieved only at the cost of allowing some combination of the two scalar fields to carry a negative energy flux.

²⁷Actually, in the case of the Cassini data, as it is quite plausible that the *positive* value of the published central value $\bar{\gamma}^{\text{Cassini}} = +2.1 \times 10^{-5}$ is due to unsubtracted systematic effects, we use $\sigma_{\gamma}^{\text{Cassini}} = 2.3 \times 10^{-5}$ but $\bar{\gamma}^{\text{Cassini}} = 0$. Otherwise, we would get unreasonably strong 1σ limits on α_0^2 because tensor-scalar theories predict that $\bar{\gamma}$ must be *negative*, see Eqs. (A.5.22) and (A.5.23).

ysis in the framework of the $T_1(\alpha_0, \beta_0)$ space of theories allows one to compare and contrast the probing powers of solar-system tests versus binary-pulsar tests (while comparing also solar-system tests among themselves and binary-pulsar ones among themselves). The result of the recent analysis (62) is shown in Figure A.3.

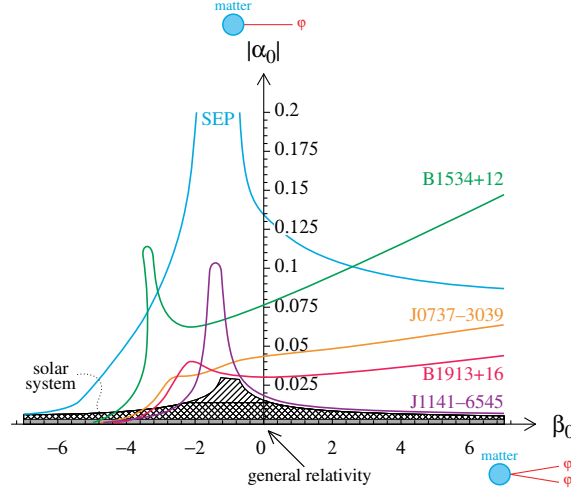


Figure A.3: Solar-system and binary-pulsar constraints on the two-parameter family of tensor-mono-scalar theories $T_1(\alpha_0, \beta_0)$. Figure taken from (62).

In Fig. A.3, the various solar-system constraints (A.5.49)–(A.5.52) are concentrated around the horizontal β_0 axis. In particular, the high-precision Cassini constraint is the lower small grey strip. The various pulsar constraints are labelled by the name of the pulsar, except for the strong equivalence principle constraint which is labelled SEP. Note that General Relativity corresponds to the origin of the (α_0, β_0) plane, and is compatible with all existing tests.

The global constraint obtained by combining all the pulsar tests would, to a good accuracy, be obtained by intersecting the various pulsar-allowed regions. One can then see on Fig. A.3 that it would be comparable to the pre-Cassini solar-system constraints and that its boundaries would be defined successively (starting from the left) by 1913+16, 1141–6545, 0737–3039, 1913+16 again and 1141–6545 again.

A first conclusion is therefore that, at the *quantitative level*, binary-pulsar tests constrain tensor-scalar gravity theories as strongly as most solar-system tests (excluding the exceptionally accurate Cassini result which constrains α_0^2 to be smaller than 1.15×10^{-5} , i.e. $|\alpha_0| < 3.4 \times 10^{-3}$). A second conclusion is obtained by comparing the behaviour of the solar-system exclusion plots and of the binary-pulsar ones around the negative β_0 axis. One sees that binary-pulsar tests exclude a whole domain of the theory space (located on

the left of $\beta_0 < -4$) which is compatible with all solar-system experiments (even when including the very tight Cassini constraint). This remarkable *qualitative* feature of pulsar tests is a direct consequence of the existence of (non-perturbative) *strong-field effects* which start developing when the product $-\beta_0 c_A$ (with c_A denoting, as above, the compactness of the pulsar) becomes of order unity.

A.6. Motion and radiation of binary black holes: post-Newtonian-expanded results

In Section A.2 we mentioned that the 2.5PN accurate equations of motion (A.2.7) were sufficiently accurate to interpret binary pulsar observations. By contrast, the forthcoming observations of gravitational wave signals from inspiralling binary black holes (and also inspiralling binary neutron stars, or mixed black-hole-neutron-star systems) has posed to theorists the double challenge of: (i) deriving more accurate equations of motion, and (ii) deriving accurate expressions for the waveforms emitted by inspiralling, and even coalescing, compact binaries. Indeed, the premier targets for LIGO/VIRGO/GEO are the waveforms emitted during the late inspiral phase of compact binaries, as well as during the subsequent ‘plunge’ and ‘merger’ phases. During these phases the basic PN expansion parameter $\gamma_e \equiv GM/c^2 D \sim (v_{\text{orbital}}/c)^2$ ceases to be numerically very small, and starts approaching values of order unity. It might then seem hopeless to tackle the motion and radiation of such close binary systems by means of a PN-expansion-type analytical approach. However, there are two reasons why it is meaningful, and probably very useful, to tackle the motion of close compact binaries by an analytical approach.

The first reason is the need to describe with high accuracy the phasing of the gravitational waveforms emitted during the inspiral phase (i.e. before the plunge and merger). During the inspiral phase, the PN expansion parameter γ_e stays most of the time significantly below 1, though it increases to reach values of order $\sim \frac{1}{6}$ at the end of the inspiral. It is then a priori reasonable to expect that the expansions of interesting physical quantities in powers of γ_e will converge sufficiently rapidly during most of the inspiral to allow one to deduce physically meaningful results from a PN expansion truncated at a large enough order. This motivated the efforts of several groups for deriving equations of motion more accurate than the 2.5PN level mentioned above, and for deriving correspondingly accurate gravitational-wave generation formalisms. These efforts will be briefly reviewed in this Section.

The second reason is that there might be ways of *improving the convergence* of PN expansions by using *resummation methods*. Two such methods have been particularly studied: one based on Padé approximants, and the other one on a novel approach to the dynamics of compact binaries called the ‘ef-

fective one body' approach.

Before discussing (in the next Section) these two resummation techniques, let us briefly recall the state of the art in analytical approaches to the motion and radiation of binary black holes²⁸.

Two different *gravitational-wave generation formalisms* have been developed up to a high PN accuracy: (i) the Blanchet-Damour-Iyer formalism (96; 97; 98; 99; 100; 101; 102) combines a multipolar post-Minkowskian (MPM) expansion in the exterior zone with a post-Newtonian expansion in the near zone; while (ii) the Will-Wiseman-Pati formalism (103; 104; 105; 106) uses a direct integration of the relaxed Einstein equations. These formalisms were used to compute increasingly accurate estimates of the gravitational waveforms emitted by inspiralling binaries. These estimates include both normal, near-zone generated post-Newtonian effects (at the 1PN (97), 2PN (107; 108; 103), and 3PN (109; 110) levels), and more subtle, wave-zone generated (linear and non-linear) 'tail effects' (100; 111; 112; 102). However, technical problems arose at the 3PN level. The representation of black holes by 'delta-function' sources causes the appearance of dangerously divergent integrals in the 3PN multipole moments. The use of Hadamard (*partie finie*) regularization did not allow one to unambiguously compute the needed 3PN-accurate quadrupole moment. Only the use of the (formally) diffeomorphism-invariant *dimensional regularization* method (i.e. analytic continuation in the dimension of space d) allowed one to complete the 3PN-level gravitational-radiation formalism (113).

In parallel with the development of 3PN-accurate gravitational radiation formalisms, several groups (notably Jaranowski-Schäfer and Blanchet-Faye) extended the PN-type computation of the equations of motion of binary black holes beyond the 2.5PN level recalled in Section A.2 above. Here also, the representation of black holes by delta-function sources and the use of the (non diffeomorphism invariant) Hadamard regularization method led to ambiguities in the computation of the badly divergent integrals that enter the 3PN equations of motion (114; 115). By contrast, the use of the (diffeomorphism invariant) *dimensional regularization* method allowed one to complete the determination of the 3PN-level equations of motion (116; 117). They have also been derived by an Einstein-Infeld-Hoffmann-type surface-integral approach (118). The 3.5PN terms in the equations of motion are also known (106; 119; 120).

The works mentioned in this Section (see (121) for a detailed account and more references) finally lead to PN-expanded results for the motion and radiation of binary black holes. For instance, the equations of motion are given

²⁸For simplicity, we shall phrase the results in the context of binary *black holes*. Actually, we use the 'effacement of internal structure' mentioned above to skeletonize the black holes by means of delta-function sources. This means that, apart from quadrupole-deformation effects, the results are also valid for binary systems comprising neutron stars.

in a form which generalize those of Section A.2 above, namely ($a = 1, 2$; $i = 1, 2, 3$)

$$\frac{d^2 z_a^i}{dt^2} = A_a^{i\text{cons}} + A_a^{iRR}, \quad (\text{A.6.1})$$

where

$$A^{\text{cons}} = A_0 + c^{-2}A_2 + c^{-4}A_4 + c^{-6}A_6, \quad (\text{A.6.2})$$

denotes the ‘conservative’ 3PN-accurate terms, while

$$A^{RR} = c^{-5}A_5 + c^{-7}A_7, \quad (\text{A.6.3})$$

denotes the time-asymmetric contributions, linked to ‘radiation reaction’.

On the other hand, if we consider for simplicity the inspiralling motion of a quasi-circular binary system, the essential quantity describing the emitted gravitational waveform is the *phase* ϕ of the quadrupolar gravitational wave amplitude $h(t) \simeq a(t) \cos(\phi(t) + \delta)$. PN theory allows one to derive several different functional expressions for the gravitational wave phase ϕ , as a function either of time or of the instantaneous frequency. For instance, as a function of time, ϕ admits the following explicit expansion in powers of $\theta \equiv \nu c^3(t_c - t)/5GM$ (where t_c denotes a formal ‘time of coalescence’, $M \equiv m_1 + m_2$ and $\nu \equiv m_1 m_2 / M^2$)

$$\phi(t) = \phi_c - \nu^{-1} \theta^{5/8} \left(1 + \sum_{n=2}^7 (a_n + a'_n \ln \theta) \theta^{-n/8} \right), \quad (\text{A.6.4})$$

with some numerical coefficients a_n, a'_n which depend only on the dimensionless (symmetric) mass ratio $\nu \equiv m_1 m_2 / M^2$. The derivation of the 3.5PN-accurate expansion (A.6.4) uses both the 3PN-accurate conservative acceleration (A.6.2) and a 3.5PN extension of the (fractionally) 1PN-accurate radiation reaction acceleration (A.6.3) obtained by assuming a balance between the energy of the binary system and the gravitational-wave energy flux at infinity (see, e.g., (121)).

A.7. Motion and radiation of binary black holes: the Effective One Body approach

The PN-expanded results briefly reviewed in the previous Section are expected to yield accurate descriptions of the motion and radiation of binary black holes during their *inspiralling* stage, say up to the moment where the PN expansion parameter $\gamma_e = GM/c^2 D$ reaches the value $\sim \frac{1}{6}$ where the orbital motion is expected to become dynamically unstable (‘last stable (circular) orbit’ and beginning of a ‘plunge’ leading to the merger of the two black holes). One possible strategy for having a complete description of the motion

and radiation of binary black holes, covering all the stages (inspiral, plunge, merger, ring-down), would then be to try to ‘stitch together’ PN-expanded analytical results describing the inspiral phase with $3d$ numerical results describing the end of the inspiral, the plunge, the merger and the ring-down of the final black hole.

However, we wish to argue that it might be possible to do a better use of all the analytical information contained in the PN-expanded results (A.6.1)-(A.6.3). The basic claim (first made in (16; 17)) is that the use of suitable *resummation methods* should allow one to describe, by analytical tools²⁹, a *sufficiently accurate* approximation of the *entire waveform*, from inspiral to ring-down, including the non-perturbative plunge and merger phases. To reach such a goal, one needs to make use of several tools: (i) resummation methods, (ii) exploitation of the flexibility of analytical approaches, (iii) extraction of the non-perturbative information contained in various numerical simulations, (iv) qualitative understanding of the basic physical features which determine the waveform.

Before coming to grasp with some of these issues, let us emphasize some conceptual aspects of this programme. Recently, an important breakthrough in numerical relativity (122; 123; 124; 125; 126; 127) has led to the computation of the gravitational waveform emitted during the late inspiral, plunge, merger and ring-down of equal-mass ($\nu = \frac{1}{4}$), non-spinning binary black holes. Some sample numerical simulations have also begun to explore the multi-parameter space of coalescing unequal-mass ($0 < \nu < \frac{1}{4}$), spinning (\vec{S}_1, \vec{S}_2) black hole binaries (see, e.g., (128; 129)). In spite of the high computer power used in these simulations, the calculation of one waveform, corresponding to specific values of the continuous parameters ($\nu, \hat{a}_1, \theta_1, \varphi_1, \hat{a}_2, \theta_2, \varphi_2$) parametrizing the considered initial binary state, takes a long time. It would be therefore extremely useful, for detection purposes, to have in hand a (quasi-)analytical approach which would combine the crucial non-perturbative information that we can get from numerical simulations, with the rich perturbative information that has been acquired in many years of work on the theory of the motion and radiation of binary black holes. The claim here is that the Effective One Body (EOB) approach offers enough *flexibility* in its definition and implementation to be able to smoothly combine these two types of information. First results towards this goal are given in Refs. (130; 131; 132; 133; 134; 135).

Let us start by discussing the first tool used in the EOB approach: the

²⁹Here we use the adjective ‘analytical’ for methods that solve explicit (analytically given) ordinary differential equations (ODE), even if one uses standard (Runge-Kutta-type) numerical tools to solve them. The important point is that, contrary to $3d$ numerical relativity simulations, numerically solving ODE’s is extremely fast, and can therefore be done (possibly even in real time) for a dense sample of theoretical parameters, such as orbital ($\nu = m_1 m_2 / M, \dots$) or spin ($\hat{a}_1 = S_1 / Gm_1^2, \theta_1, \varphi_1, \dots$) parameters.

systematic use of resummation methods. Two such methods have been employed (and combined), and some evidence has been given that they do significantly improve the convergence properties of PN expansions. The first method is the use of *Padé approximants*. It has been shown in Ref. (12) that near-diagonal Padé approximants of the radiation reaction force \mathcal{F} ³⁰ seemed to provide a good representation of \mathcal{F} down to the last stable orbit (which is expected to occur when $D \sim 6GM/c^2$, i.e. when $\gamma_e \simeq \frac{1}{6}$). The second method is a novel approach to the dynamics of compact binaries, which constitutes the core of the Effective One Body (EOB) method. The EOB method was introduced in (16; 17), and was further extended to the 3PN level in (136), and by including spin effects in (137).

For simplicity of exposition, let us first explain the EOB method at the 2PN level. The starting point of the method is the 2PN-accurate Hamiltonian describing (in Arnowitt-Deser-Misner-type coordinates) the conservative, or time symmetric, part of the equations of motion (A.2.8) (i.e. the truncation $A^{\text{cons}} = A_0 + c^{-2}A_2 + c^{-4}A_4$ of Eq. (A.6.2)) say $H_{2\text{PN}}(\mathbf{q}_1 - \mathbf{q}_2, \mathbf{p}_1, \mathbf{p}_2)$. By going to the center of mass of the system ($\mathbf{p}_1 + \mathbf{p}_2 = 0$), one obtains a PN-expanded Hamiltonian describing the *relative motion*, $\mathbf{q} = \mathbf{q}_1 - \mathbf{q}_2$, $\mathbf{p} = \mathbf{p}_1 = -\mathbf{p}_2$:

$$H_{2\text{PN}}^{\text{relative}}(\mathbf{q}, \mathbf{p}) = H_0(\mathbf{q}, \mathbf{p}) + \frac{1}{c^2} H_2(\mathbf{q}, \mathbf{p}) + \frac{1}{c^4} H_4(\mathbf{q}, \mathbf{p}), \quad (\text{A.7.1})$$

where $H_0(\mathbf{q}, \mathbf{p}) = \frac{1}{2\mu} \mathbf{p}^2 + \frac{GM\mu}{|\mathbf{q}|}$ (with $M \equiv m_1 + m_2$ and $\mu = m_1 m_2 / M$) corresponds to the Newtonian approximation to the relative motion, while H_2 describes 1PN corrections and H_4 2PN ones. It is well known that, at the Newtonian approximation, $H_0(\mathbf{q}, \mathbf{p})$ can be thought of as describing a ‘test particle’ of mass μ orbiting around an ‘external mass’ GM . The EOB approach is a *general relativistic generalization* of this fact. It consists in looking for an ‘external spacetime geometry’ $g_{\mu\nu}^{\text{ext}}(x^\lambda; GM)$ such that the geodesic dynamics of a ‘test particle’ of mass μ within $g_{\mu\nu}^{\text{ext}}(x^\lambda, GM)$ is *equivalent*³¹ (when expanded in powers of $1/c^2$) to the original, relative PN-expanded dynamics (A.7.1). The advantage of the EOB method is that it *compactifies* the information contained in the rather complicated PN-expanded Hamiltonian (A.7.1) into the much simpler PN-expansions of the two independent metric coeffi-

³⁰We henceforth denote by \mathcal{F} the *Hamiltonian* version of the radiation reaction term A^{RR} , Eq. (A.6.3), in the (PN-expanded) equations of motion. It can be heuristically computed up to (absolute) 5.5PN (109; 138; 113) and even 6PN (143) order by assuming that the energy radiated in gravitational waves at infinity is balanced by a loss of the dynamical energy of the binary system.

³¹See the above references to see the precise sense in which the two dynamics are equivalent. Let us just say here that the best way to think about it is to think of both dynamics in *quantum terms* as two sets of quantized energy spectra $E_{2\text{PN}}^{\text{relative}}(n, \ell)$, $E_{\text{ext}}(n, \ell)$ that are required to be mapped onto each other by an energy rescaling $E_{2\text{PN}}^{\text{relative}} = f(E_{\text{ext}})$.

icients $A(R)$, $B(R)$ of the ‘external’ geometry

$$g_{\mu\nu}^{\text{ext}} dx^\mu dx^\nu = -A(R) c^2 dT^2 + B(R) dR^2 + R^2(d\theta^2 + \sin^2\theta d\varphi^2). \quad (\text{A.7.2})$$

For instance, the crucial ‘ g_{00}^{ext} ’ metric coefficient $A(R)$ (which fully encodes the energetics of circular orbits) is originally given, at 2PN order, by the PN expansion

$$A_{2\text{PN}}(R) = 1 - 2u + 2\nu u^3, \quad (\text{A.7.3})$$

where $u \equiv GM/c^2R$ and $\nu \equiv \mu/M \equiv m_1 m_2 / (m_1 + m_2)^2$.

The dimensionless parameter $\nu \equiv \mu/M$ varies between 0 (in the test mass limit $m_1 \ll m_2$) and $\frac{1}{4}$ (in the equal-mass case $m_1 = m_2$). When $\nu \rightarrow 0$, Eq. (A.7.3) yields back, as expected, the well-known Schwarzschild time-time metric coefficient $-g_{00}^{\text{Schw}} = 1 - 2u = 1 - 2GM/c^2R$. One therefore sees in Eq. (A.7.3) the rôle of ν as a deformation parameter connecting a well-known test-mass result to a non trivial and new 2PN result. It is also to be noted that the 1PN EOB result $A_{1\text{PN}}(R) = 1 - 2u$ happens to be ν -independent, and therefore identical to $A^{\text{Schw}} = 1 - 2u$. This is remarkable in view of the many non-trivial ν -dependent terms in the 1PN relative dynamics. The physically real 1PN ν -dependence happens to be fully encoded in the function $f(E)$ mapping the two energy spectra which was found to be always given by a very simple result:

$$E_{\text{EOB}} = E_{\text{real}} \left(1 + \frac{1}{2} \frac{E_{\text{real}}}{Mc^2} \right). \quad (\text{A.7.4})$$

Let us emphasize the remarkable simplicity of the 2PN result (A.7.3). The 2PN Hamiltonian (A.7.1) contains eleven rather complicated ν -dependent terms. After transformation to the EOB format, the dynamical information contained in these eleven coefficients gets *compactified* into the very simple additional contribution $+2\nu u^3$ in $A(R)$, together with an equally simple contribution in the radial metric coefficient: $(A(R)B(R))_{2\text{PN}} = 1 - 6\nu u^2$. This compactification process is even more drastic when one goes to the next (conservative) post-Newtonian order: the 3PN level, i.e. additional terms of order $\mathcal{O}(1/c^6)$ in the Hamiltonian (A.7.1). As mentioned above, the complete obtention of the 3PN dynamics has represented quite a theoretical challenge and the final, resulting Hamiltonian is quite complicated. Even after going to the center of mass frame, the 3PN additional contribution $\frac{1}{c^6} H_6(\mathbf{q}, \mathbf{p})$ to Eq. (A.7.1) introduces eleven new complicated ν -dependent coefficients. After transformation to the EOB format (16), these eleven new coefficients get ‘compactified’ into only *three* additional terms: (i) an additional contribution to $A(R)$, (ii) an additional contribution to $B(R)$, and (iii) a $\mathcal{O}(\mathbf{p}^4)$ modification of the ‘external’ geodesic Hamiltonian. For instance, the crucial 3PN g_{00}^{ext}

metric coefficient becomes

$$A_{3\text{PN}}(R) = 1 - 2u + 2\nu u^3 + a_4 \nu u^4, \quad (\text{A.7.5})$$

where

$$a_4 = \frac{94}{3} - \frac{41}{32} \pi^2 \simeq 18.6879027. \quad (\text{A.7.6})$$

The fact that the 3PN coefficient a_4 in the crucial ‘effective radial potential’ $A_{3\text{PN}}(R)$, Eq. (A.7.5), is rather large and positive indicates that the ν -dependent nonlinear gravitational effects lead, for comparable masses ($\nu \sim \frac{1}{4}$), to a last stable (circular) orbit (LSO) which has a higher frequency and a larger binding energy than what a naive scaling from the test-particle limit ($\nu \rightarrow 0$) would suggest. Actually, the PN-expanded form (A.7.5) of $A_{3\text{PN}}(R)$ does not seem to be a good representation of the (unknown) exact function $A_{\text{EOB}}(R)$ when the (Schwarzschild-like) relative coordinate R becomes smaller than about $6GM/c^2$ (which is the radius of the LSO in the test-mass limit). It was therefore suggested (136) to further resum³² $A_{3\text{PN}}(R)$ by replacing it by a suitable Padé (P) approximant. For instance, the replacement of $A_{3\text{PN}}(R)$ by

$$A_3^1(R) \equiv P_3^1[A_{3\text{PN}}(R)] = \frac{1 + n_1 u}{1 + d_1 u + d_2 u^2 + d_3 u^3} \quad (\text{A.7.7})$$

ensures that the $\nu = \frac{1}{4}$ case is smoothly connected with the $\nu = 0$ limit.

The use of (A.7.7) was suggested before one had any (reliable) non-perturbative information on the binding of close black hole binaries. Later, a comparison with some ‘waveless’ numerical simulations of circular black hole binaries (130) has given some evidence that (A.7.7) is physically adequate. There it was also emphasized that, in principle, the comparison between numerical data and EOB-based predictions should allow one to determine the effect of the unknown higher PN contributions to Eq. (A.7.5). For instance, one can add a 4PN-like term $+ a_5 \nu u^5$ in Eq. (A.7.5), and then Padé the resulting radial function, say $A_4^1 = P_4^1[A_{3\text{PN}} + a_5 \nu u^5]$. Comparing the predictions of $A_4^1[a_5]$ to numerical data might then determine what is the physically preferred ‘effective’ value of the unknown coefficient a_5 . This is an example of the useful *flexibility* of analytical approaches: the fact that one can tap numerically-based, non-perturbative information to improve the EOB approach.

As recently emphasized (134), it is quite useful to tap the information contained in the Regge-Wheeler-Zerilli-type signals emitted by test-particles orbiting black holes (small ν limit). The numerical methods needed to compute these non-perturbative phenomena (139; 140; 133) are much simpler than the

³²The PN-expanded EOB building blocks $A(R), B(R), \dots$ already represent a *resummation* of the PN dynamics in the sense that they have compactified the many terms of the original PN-expanded Hamiltonian within a very concise format. But one should not refrain to further resum the EOB building blocks themselves, if this is physically motivated.

ones needed in the comparable-mass case ($\nu \sim \frac{1}{4}$), but their results contain a lot of useful physical insights, which are relatively easy to explore.

Let us finally sketch the overall structure of the EOB approach to the motion and radiation of binary black holes. Two of the basic elements are the EOB Hamiltonian $H_{\text{EOB}}(\mathbf{q}, \mathbf{p}, \mathbf{S}_1, \mathbf{S}_2)$ and the radiation reaction force $\mathcal{F}(\mathbf{q}, \mathbf{p}, \mathbf{S}_1, \mathbf{S}_2)$. We have indicated here that the EOB approach has been generalized to the case of arbitrarily spinning black holes (137; 144; 141). This leads to ODE's for the evolution of the variables $\mathbf{q}, \mathbf{p}, \mathbf{S}_1$ and \mathbf{S}_2 :

$$\begin{aligned} \frac{d\mathbf{q}}{dt} &= \frac{\partial H_{\text{EOB}}}{\partial \mathbf{p}}, \\ \frac{d\mathbf{p}}{dt} &= -\frac{\partial H_{\text{EOB}}}{\partial \mathbf{q}} + \mathcal{F}, \\ \frac{d\mathbf{S}_1}{dt} &= \frac{\partial H_{\text{EOB}}}{\partial \mathbf{S}_1} \times \mathbf{S}_1, \quad \frac{d\mathbf{S}_2}{dt} = \frac{\partial H_{\text{EOB}}}{\partial \mathbf{S}_2} \times \mathbf{S}_2. \end{aligned} \quad (\text{A.7.8})$$

The knowledge of the time evolution of $\mathbf{q}(t), \mathbf{p}(t), \mathbf{S}_1(t), \mathbf{S}_2(t)$ is then injected into some gravitational-wave generation formalism, $h_{ij}(t) = H_{ij}(\mathbf{q}, \mathbf{p}, \mathbf{S}_1, \mathbf{S}_2)$, and used to compute the waveform $h_{ij}^{\text{insp}}(t)$ during *inspiral and plunge*, up to some 'matching' time t_m . [The analytical prediction $H_{ij}(\mathbf{q}, \mathbf{p}, \mathbf{S}_1, \mathbf{S}_2)$ can be computed with various accuracies: Ref. (17) used the lowest-order quadrupole approximation, while Ref. (134) uses a 3PN-accurate, resummed quadrupolar waveform.] Then, one continues this waveform to the merger and ring-down phase by smoothly matching, around the matching time t_m , the EOB-dynamics derived $h_{ij}^{\text{insp}}(t)$ to a pure ring-down waveform, made of the superposition of several quasi-normal-mode frequencies: $h^{\text{ring}}(t) = \sum_n c_n e^{-\sigma_n(t-t_m)}$, with $\sigma_n = \alpha_n + i\omega_n$. Finally, this procedure defines a complete, quasi-analytical EOB-based waveform (covering the full process from inspiral to ring-down) as:

$$\begin{aligned} h^{\text{EOB}}(t) &= \theta(t_m - t) H_{ij}(\mathbf{q}(t), \mathbf{p}(t), \mathbf{S}_1(t), \mathbf{S}_2(t)) \\ &+ \theta(t - t_m) \sum_n c_n^{\text{matched}} e^{-\sigma_n(t-t_m)}, \end{aligned} \quad (\text{A.7.9})$$

where $\theta(t)$ denotes Heaviside's step function.

The lowest approximation to the complete EOB waveform was constructed in (17). Since then, more accurate versions were constructed in (144; 134). These EOB-type waveforms have been compared to full, 3d numerical relativity waveforms in (131; 142). When taking advantage of the flexibility available in the EOB approach, an excellent agreement is reached between the quasi-analytical EOB-based waveforms and the numerical relativity ones.

A.8. Conclusions

In conclusion, we hope to have exemplified the way compact binaries set theoretical challenges to General Relativity.

On the one hand, over the past thirty years, binary pulsars have stimulated a lively dialogue between Experiment and Theory. This dialogue has led to novel tests of General Relativity, which have confirmed, with high accuracy, some of the strong-field and radiative aspects of Einstein's theory. The recent discovery of a *double* binary pulsar has greatly increased the number of available strong-field tests of General Relativity.

On the other hand, the forthcoming detection of gravitational-wave signals in large interferometers is currently stimulating both analytical and numerical investigations in inspiralling and coalescing binary black holes. For the moment, this fosters a dialogue between numerical results and analytical methods. Hopefully, one will soon be able to compare the combined analytical-numerical predictions to real gravitational wave data.

Bibliography

- [1] T. Damour, “Black Hole and Neutron Star Binaries: Theoretical Challenges,” arXiv:0705.3109 [gr-qc]. 53 pages, 3 eps figures, to appear in a revised edition of the book: Neutron Stars, Black Holes and Binary X-Ray Sources by H. Gursky and R. Ruffini
- [2] A. Buonanno and T. Damour, Phys. Rev. D **59**, 084006 (1999) [arXiv:gr-qc/9811091].
- [3] A. Buonanno and T. Damour, Phys. Rev. D **62**, 064015 (2000) [arXiv:gr-qc/0001013].
- [4] T. Damour, P. Jaranowski and G. Schaefer, Phys. Rev. D **62**, 084011 (2000) [arXiv:gr-qc/0005034].
- [5] T. Damour, Phys. Rev. D **64**, 124013 (2001) [arXiv:gr-qc/0103018].
- [6] F. Pretorius, arXiv:0710.1338 [gr-qc].
- [7] T. Damour and A. Nagar, Phys. Rev. D **76**, 064028 (2007) [arXiv:0705.2519 [gr-qc]].
- [8] M. Davis, R. Ruffini and J. Tiomno, Phys. Rev. D **5**, 2932 (1972).
- [9] Y. Pan *et al.*, arXiv:0704.1964 [gr-qc].
- [10] T. Damour and A. Nagar, Phys. Rev. D **76**, 044003 (2007) [arXiv:0704.3550 [gr-qc]].
- [11] A. Buonanno, Y. Pan, J. G. Baker, J. Centrella, B. J. Kelly, S. T. McWilliams and J. R. van Meter, arXiv:0706.3732 [gr-qc].
- [12] T. Damour, B. R. Iyer and B. S. Sathyaprakash, Phys. Rev. D **57**, 885 (1998) [arXiv:gr-qc/9708034].
- [13] M. Boyle *et al.*, arXiv:0710.0158 [gr-qc].
- [14] T. Damour and A. Nagar, Comparing Effective-One-Body gravitational waveforms to accurate numerical data, arXiv:0711.2628 [gr-qc], submitted to Physical Review D.
- [15] R. A. Hulse, J. H. Taylor: Discovery of a pulsar in a binary system, *Astrophys. J.* **195**, L51 (1975).

- [16] A. Buonanno, T. Damour: Effective one-body approach to general relativistic two-body dynamics, *Phys. Rev. D* **59**, 084006 (1999), arXiv:gr-qc/9811091.
- [17] A. Buonanno, T. Damour: Transition from inspiral to plunge in binary black hole coalescences, *Phys. Rev. D* **62**, 064015 (2000), arXiv:gr-qc/0001013.
- [18] F. K. Manasse: *J. Math. Phys.* **4**, 746 (1963).
- [19] P. D. D'Eath: *Phys. Rev. D* **11**, 1387 (1975).
- [20] R. E. Kates: *Phys. Rev. D* **22**, 1853 (1980).
- [21] D. M. Eardley: *Astrophys. J.* **196**, L59 (1975).
- [22] C. M. Will, D. M. Eardley: *Astrophys. J.* **212**, L91 (1977).
- [23] T. Damour: *Gravitational radiation and the motion of compact bodies*, in *Gravitational Radiation*, edited by N. Deruelle and T. Piran, North-Holland, Amsterdam, pp. 59-144 (1983).
- [24] K. S. Thorne, J. B. Hartle: Laws of motion and precession for black holes and other bodies, *Phys. Rev. D* **31**, 1815 (1984).
- [25] C. M. Will: *Theory and experiment in gravitational physics*, Cambridge University Press (1993) 380 p.
- [26] S.M. Kopeikin: Celestial coordinate reference systems in curved space-time, *Celestial Mechanics*, **44**, 87 (1988); V. A. Brumberg, S. M. Kopeikin: *Nuovo Cimento B* **103**, 63 (1988).
- [27] T. Damour, M. Soffel, C. M. Xu: General relativistic celestial mechanics. 1. Method and definition of reference system, *Phys. Rev. D* **43**, 3273 (1991); General relativistic celestial mechanics. 2. Translational equations of motion, *Phys. Rev. D* **45**, 1017 (1992); General relativistic celestial mechanics. 3. Rotational equations of motion, *Phys. Rev. D* **47**, 3124 (1993); General relativistic celestial mechanics. 4. Theory of satellite motion, *Phys. Rev. D* **49**, 618 (1994).
- [28] G. 't Hooft , M. J. G. Veltman: Regularization and renormalization of gauge fields, *Nucl. Phys. B* **44**, 189 (1972).
- [29] T. Damour, G. Esposito-Farèse: Gravitational-wave versus binary-pulsar tests of strong-field gravity, *Phys. Rev. D* **58**, 042001 (1998), gr-qc/9803031.

-
- [30] W.D. Goldberger, I.Z. Rothstein: An effective field theory of gravity for extended objects, *Phys. Rev. D* **73** (2006) 104029; arXiv:hep-th/0409156.
- [31] T. Damour, N. Deruelle: Radiation reaction and angular momentum loss in small angle gravitational scattering, *Phys. Lett. A* **87**, 81 (1981).
- [32] T. Damour: Problème des deux corps et freinage de rayonnement en relativité générale, *C.R. Acad. Sci. Paris, Série II*, **294**, 1355 (1982).
- [33] T. Damour: The problem of motion in Newtonian and Einsteinian gravity, in *Three Hundred Years of Gravitation*, edited by S.W. Hawking and W. Israel, Cambridge University Press, Cambridge, pp. 128-198 (1987).
- [34] T. Damour, N. Deruelle: General relativistic celestial mechanics of binary systems I. The post-Newtonian motion, *Ann. Inst. Henri Poincaré* **43**, 107 (1985).
- [35] T. Damour: Gravitational radiation reaction in the binary pulsar and the quadrupole formula controversy, *Phys. Rev. Lett.* **51**, 1019 (1983).
- [36] R. Blandford, S. A. Teukolsky: *Astrophys. J.* **205**, 580 (1976).
- [37] T. Damour, N. Deruelle: General relativistic celestial mechanics of binary systems II. The post-Newtonian timing formula, *Ann. Inst. Henri Poincaré* **44**, 263 (1986).
- [38] S.M. Kopeikin: On possible implications of orbital parallaxes of wide orbit binary pulsars and their measurability, *Astrophysical Journal (Letters)* **439** pp. L5-L8 (1995); S.M. Kopeikin: Proper Motion of Binary Pulsars as a Source of Secular Variations of Orbital Parameters, *Astrophysical Journal (Letters)* **467** pp. L93-L95 (1996).
- [39] W. van Straten, M. Bailes, M. C. Britton, S. R. Kulkarni, S. B. Anderson, R. N. Manchester and J. Sarkissian: A test of general relativity from the three-dimensional orbital geometry of a binary pulsar, *Nature* **412**, 158 (2001) [arXiv:astro-ph/0108254].
- [40] S.M. Kopeikin, G. Schäfer: Lorentz covariant theory of light propagation in gravitational fields of arbitrary-moving bodies, *Phys. Rev. D* **60**, 124002 (1999), arXiv:gr-qc/9902030.
- [41] T. Damour, J. H. Taylor: Strong field tests of relativistic gravity and binary pulsars, *Phys. Rev. D* **45**, 1840 (1992).

- [42] T. Damour: Strong-field tests of general relativity and the binary pulsar, in *Proceedings of the 2cd Canadian Conference on General Relativity and Relativistic Astrophysics*, edited by A. Coley, C. Dyer, T. Tupper, World Scientific, Singapore, pp. 315-334 (1988).
- [43] T. Damour, G. Esposito-Farèse: Tensor-multi-scalar theories of gravitation, *Class. Quant. Grav.* **9**, 2093 (1992).
- [44] T. Damour, G. Esposito-Farèse: Non-perturbative strong-field effects in tensor-scalar theories of gravitation, *Phys. Rev. Lett.* **70**, 2220 (1993).
- [45] T. Damour, G. Esposito-Farèse: Tensor-scalar gravity and binary-pulsar experiments, *Phys. Rev. D* **54**, 1474 (1996), arXiv:gr-qc/9602056.
- [46] J. M. Weisberg, J. H. Taylor: Relativistic binary pulsar B1913+16: thirty years of observations and analysis, To appear in the proceedings of Aspen Winter Conference on Astrophysics: Binary Radio Pulsars, Aspen, Colorado, 11-17 Jan 2004., arXiv:astro-ph/0407149.
- [47] T. Damour, J. H. Taylor: On the orbital period change of the binary pulsar Psr-1913+16, *The Astrophysical Journal* **366**, 501 (1991).
- [48] C. M. Will, H. W. Zaglauer: Gravitational radiation, close binary systems, and the Brans-Dicke theory of gravity, *Astrophys. J.* **346**, 366 (1989).
- [49] J. H. Taylor, A. Wolszczan, T. Damour, J. M. Weisberg: Experimental constraints on strong field relativistic gravity, *Nature* **355**, 132 (1992).
- [50] I. H. Stairs, S. E. Thorsett, J. H. Taylor, A. Wolszczan: Studies of the relativistic binary pulsar PSR B1534+12: I. Timing analysis, *Astrophys. J.* **581**, 501 (2002).
- [51] K. Nordtvedt: Equivalence principle for massive bodies. 2. Theory, *Phys. Rev.* **169**, 1017 (1968).
- [52] T. Damour, G. Schäfer: New tests of the strong equivalence principle using binary pulsar data, *Phys. Rev. Lett.* **66**, 2549 (1991).
- [53] I. H. Stairs *et al.*: Discovery of three wide-orbit binary pulsars: implications for binary evolution and equivalence principles, *Astrophys. J.* **632**, 1060 (2005).
- [54] N. Wex: New limits on the violation of the Strong Equivalence Principle in strong field regimes, *Astronomy and Astrophysics* **317**, 976 (1997), gr-qc/9511017.

-
- [55] V. M. Kaspi *et al.*: Discovery of a young radio pulsar in a relativistic binary orbit, arXiv:astro-ph/0005214.
- [56] M. Bailes, S. M. Ord, H. S. Knight, A. W. Hotan: Self-consistency of relativistic observables with general relativity in the white dwarf-neutron star binary pulsar PSR J1141-6545, *Astrophys. J.* **595**, L49 (2003).
- [57] M. Burgay *et al.*: An increased estimate of the merger rate of double neutron stars from observations of a highly relativistic system, *Nature* **426**, 531 (2003), arXiv:astro-ph/0312071.
- [58] A. G. Lyne *et al.*: A double-pulsar system: A rare laboratory for relativistic gravity and plasma physics, *Science* **303**, 1153 (2004).
- [59] M. Kramer *et al.*: eConf **C041213**, 0038 (2004), astro-ph/0503386.
- [60] M. Kramer *et al.*: Tests of general relativity from timing the double pulsar, *Science* **314**, 97-102 (2006).
- [61] S. M. Ord, M. Bailes, W. van Straten: The Scintillation Velocity of the Relativistic Binary Pulsar PSR J1141-6545, arXiv:astro-ph/0204421.
- [62] T. Damour, G. Esposito-Farèse: Binary-pulsar versus solar-system tests of tensor-scalar gravity, 2007, in preparation.
- [63] T. Damour, R. Ruffini: Sur certaines vérifications nouvelles de la relativité générale rendues possibles par la découverte d'un pulsar membre d'un système binaire, *C.R. Acad. Sci. Paris (Série A)* **279**, 971 (1974).
- [64] B. M. Barker, R. F. O'Connell: Gravitational two-body problem with arbitrary masses, spins, and quadrupole moments, *Phys. Rev. D* **12**, 329 (1975).
- [65] M. Kramer: *Astrophys. J.* **509**, 856 (1998).
- [66] J. M. Weisberg, J. H. Taylor: *Astrophys. J.* **576**, 942 (2002).
- [67] I. H. Stairs, S. E. Thorsett, Z. Arzoumanian: Measurement of gravitational spin-orbit coupling in a binary pulsar system, *Phys. Rev. Lett.* **93**, 141101 (2004).
- [68] A. W. Hotan, M. Bailes, S. M. Ord: Geodetic Precession in PSR J1141-6545, *Astrophys. J.* **624**, 906 (2005).
- [69] T. Damour, G. Schäfer: Higher order relativistic periastron advances and binary pulsars, *Nuovo Cim. B* **101**, 127 (1988).

- [70] J.M. Lattimer, B.F. Schutz: Constraining the equation of state with moment of inertia measurements, *Astrophys. J.* **629**, 979 (2005), arXiv:astro-ph/0411470.
- [71] I. A. Morrison, T. W. Baumgarte, S. L. Shapiro, V. R. Pandharipande: The moment of inertia of the binary pulsar J0737-3039A: constraining the nuclear equation of state, *Astrophys. J.* **617**, L135 (2004).
- [72] A. S. Eddington: *The Mathematical Theory of Relativity*, Cambridge University Press, London (1923).
- [73] L. I. Schiff: *Am. J. Phys.* **28**, 340 (1960).
- [74] R. Baierlein: *Phys. Rev.* **162**, 1275 (1967).
- [75] C. M. Will: *Astrophys. J.* **163**, 611 (1971).
- [76] C. M. Will, K. Nordtvedt: *Astrophys. J.* **177**, 757 (1972).
- [77] C. M. Will: The confrontation between general relativity and experiment, *Living Rev. Rel.* **4**, 4 (2001) arXiv:gr-qc/0103036; update (2005) in arXiv:gr-qc/0510072.
- [78] P. Jordan: *Nature (London)* **164**, 637 (1949); *Schwerkraft und Weltall (Vieweg, Braunschweig, 1955)*; *Z. Phys.* **157**, 112 (1959).
- [79] M. Fierz: *Helv. Phys. Acta* **29**, 128 (1956).
- [80] C. Brans, R. H. Dicke: Mach's principle and a relativistic theory of gravitation, *Phys. Rev.* **124**, 925 (1961).
- [81] T. Damour, G. Esposito-Farèse: Testing gravity to second post-Newtonian order: A field theory approach, *Phys. Rev. D* **53**, 5541 (1996), arXiv:gr-qc/9506063.
- [82] T. Damour, A. M. Polyakov: The string dilaton and a least coupling principle, *Nucl. Phys. B* **423**, 532 (1994) arXiv:hep-th/9401069; *String theory and gravity, Gen. Rel. Grav.* **26**, 1171 (1994), arXiv:gr-qc/9411069.
- [83] T. Damour, D. Vokrouhlicky: The equivalence principle and the moon, *Phys. Rev. D* **53**, 4177 (1996), arXiv:gr-qc/9507016.
- [84] J. Khoury, A. Weltman: Chameleon fields: Awaiting surprises for tests of gravity in space, *Phys. Rev. Lett.* **93**, 171104 (2004), arXiv:astro-ph/0309300.
- [85] J. Khoury, A. Weltman: Chameleon cosmology, *Phys. Rev. D* **69**, 044026 (2004), arXiv:astro-ph/0309411.

-
- [86] P. Brax, C. van de Bruck, A. C. Davis, J. Khoury, A. Weltman: Detecting dark energy in orbit: The cosmological chameleon, *Phys. Rev. D* **70**, 123518 (2004), arXiv:astro-ph/0408415.
- [87] T. Damour, F. Piazza, G. Veneziano: Runaway dilaton and equivalence principle violations, *Phys. Rev. Lett.* **89**, 081601 (2002), arXiv:gr-qc/0204094; Violations of the equivalence principle in a dilaton-runaway scenario, *Phys. Rev. D* **66**, 046007 (2002), arXiv:hep-th/0205111.
- [88] T. Damour, G. Esposito-Farèse: Testing gravity to second post-Newtonian order: A field theory approach, *Phys. Rev. D* **53**, 5541 (1996), arXiv:gr-qc/9506063.
- [89] T. Damour, K. Nordtvedt: General relativity as a cosmological attractor of tensor scalar theories, *Phys. Rev. Lett.* **70**, 2217 (1993); Tensor-scalar cosmological models and their relaxation toward general relativity, *Phys. Rev. D* **48**, 3436 (1993).
- [90] J. B. Hartle: Slowly rotating relativistic stars. 1. Equations of structure, *Astrophys. J.* **150**, 1005 (1967).
- [91] G. Esposito-Farèse: Binary-pulsar tests of strong-field gravity and gravitational radiation damping, in *Proceedings of the tenth Marcel Grossmann Meeting, July 2003*, edited by M. Novello et al., World Scientific (2005), p. 647, arXiv:gr-qc/0402007.
- [92] B. Bertotti, L. Iess, P. Tortora: A test of general relativity using radio links with the Cassini spacecraft, *Nature* **425**, 374 (2003).
- [93] S. S. Shapiro *et al.*: *Phys. Rev. Lett* **92**, 121101 (2004).
- [94] I. I. Shapiro: in *General Relativity and Gravitation 12*, edited by N. Ashby, D. F. Bartlett, and W. Wyss (Cambridge University Press, 1990), p. 313.
- [95] J. G. Williams, S. G. Turyshev, D. H. Boggs: Progress in lunar laser ranging tests of relativistic gravity, *Phys. Rev. Lett.* **93**, 261101 (2004), arXiv:gr-qc/0411113.
- [96] L. Blanchet, T. Damour: Radiative gravitational fields in general relativity I. General structure of the field outside the source, *Phil. Trans. R. Soc. Lond.* **A320** (1986), pp 379-430.
- [97] L. Blanchet, T. Damour: Post-Newtonian generation of gravitational waves, *Ann. IHP* **50** (1989), pp. 377-408.

- [98] T. Damour, B.R. Iyer: Multipole analysis for electromagnetism and linearized gravity with irreducible Cartesian tensors, *Physical Review D* **43** (1991), pp. 3259-3272.
- [99] T. Damour, B.R. Iyer: Post-Newtonian generation of gravitational waves II. The spin moments., *Ann. IHP* **54** (1991), pp. 115-164.
- [100] L. Blanchet, T. Damour: Hereditary effects in gravitational radiation, *Phys. Rev. D* **46** (1992), pp. 4304-4319.
- [101] L. Blanchet: Second post-Newtonian generation of gravitational radiation, *Phys. Rev. D* **51**, 2559 (1995), arXiv:gr-qc/9501030.
- [102] L. Blanchet: Gravitational-wave tails of tails, *Class. Quant. Grav.* **15**, 113 (1998) [Erratum-ibid. **22**, 3381 (2005)], arXiv:gr-qc/9710038.
- [103] C. M. Will, A. G. Wiseman: Gravitational radiation from compact binary systems: gravitational waveforms and energy loss to second post-Newtonian order, *Phys. Rev. D* **54**, 4813 (1996), arXiv:gr-qc/9608012.
- [104] C.M. Will: Generation of post-Newtonian gravitational radiation via direct integration of the relaxed Einstein equations, *Prog. Theor. Phys. Suppl.* **136** (1999) 158-167, arXiv:gr-qc/9910057.
- [105] M.E. Pati, C.M. Will: Post-Newtonian gravitational radiation and equations of motion via direct integration of the relaxed Einstein equations. I. Foundations, *Phys. Rev. D* **62** (2000) 124015, arXiv:gr-qc/0007087.
- [106] M. E. Pati, C. M. Will: Post-Newtonian gravitational radiation and equations of motion via direct integration of the relaxed Einstein equations. II: Two-body equations of motion to second post-Newtonian order, and radiation-reaction to 3.5 post-Newton, *Phys. Rev. D* **65**, 104008 (2002), arXiv:gr-qc/0201001.
- [107] L. Blanchet, T. Damour, B. R. Iyer, C. M. Will and A. G. Wiseman: Gravitational radiation damping of compact binary systems to second post-Newtonian order, *Phys. Rev. Lett.* **74**, 3515 (1995), arXiv:gr-qc/9501027.
- [108] L. Blanchet, T. Damour, B. R. Iyer: Gravitational waves from inspiralling compact binaries: Energy loss and wave form to second post-Newtonian order, *Phys. Rev. D* **51**, 5360 (1995) [Erratum-ibid. **D 54**, 1860 (1996)], arXiv:gr-qc/9501029.

-
- [109] L. Blanchet, B.R. Iyer, B. Joguet: Gravitational waves from inspiralling compact binaries: Energy flux to third post-Newtonian order, *Phys. Rev. D* **65** (2002) 064005; Erratum-ibid. *D71* (2005) 129903, arXiv:gr-qc/0105098.
- [110] L. Blanchet, B.R. Iyer: Hadamard regularization of the third post-Newtonian gravitational wave generation of two point masses, *Phys. Rev. D* **71** (2005) 024004, arXiv:gr-qc/0409094.
- [111] A.G. Wiseman: Coalescing binary systems of compact objects to (post)^{5/2}-Newtonian order. IV. The gravitational wave tail , *Phys. Rev. D* **48**, 4757-4770 (1993).
- [112] L. Blanchet, G. Schäfer: Gravitational wave tails, *Class. Q. Grav.* (1993).
- [113] L. Blanchet, T. Damour, G. Esposito-Farèse, B.R. Iyer: Dimensional regularization of the third post-Newtonian gravitational wave generation from two point masses, *Phys. Rev. D* **71** (2005) 124004, arXiv:gr-qc/0503044.
- [114] P. Jaranowski, G. Schäfer: 3rd post-Newtonian higher order Hamilton dynamics for two-body point-mass systems, *Phys. Rev. D* **57** (1998) 7274-7291; Erratum-ibid. *D 63* (2001) 029902, arXiv:gr-qc/9712075.
- [115] L. Blanchet, G. Faye: General relativistic dynamics of compact binaries at the third post-Newtonian order, *Phys. Rev. D* **63** (2001) 062005, arXiv:gr-qc/0007051.
- [116] T. Damour, P. Jaranowski, G. Schäfer: Dimensional regularization of the gravitational interaction of point masses, *Phys. Lett. B* **513**, 147 (2001), arXiv:gr-qc/0105038.
- [117] L. Blanchet, T. Damour, G. Esposito-Farèse: Dimensional regularization of the third post-Newtonian dynamics of point particles in harmonic coordinates, *Phys. Rev. D* **69**, 124007 (2004), arXiv:gr-qc/0311052.
- [118] Y. Itoh, T. Futamase: New derivation of a third post-Newtonian equation of motion for relativistic compact binaries without ambiguity, *Phys. Rev. D* **68**, 121501(R), (2003).
- [119] C. Königsdörffer, G. Faye, G. Schäfer: Binary black-hole dynamics at the third-and-a-half post-Newtonian order in the ADM formalism, *Phys. Rev. D* **68**, 044004-1-19 (2003).
- [120] S. Nissanke, L. Blanchet: Gravitational radiation reaction in the equations of motion of compact binaries to 3.5 post-Newtonian order, *Class. Quant. Grav.* **22**, 1007 (2005), arXiv:gr-qc/0412018.

- [121] L. Blanchet: Gravitational radiation from post-Newtonian sources and inspiralling compact binaries, *Living Rev. Rel.* **5**, 3 (2002); Updated article: <http://www.livingreviews.org/lrr-2006-4>
- [122] F. Pretorius: Evolution of binary black hole spacetimes, *Phys. Rev. Lett.* **95** (2005) 121101, arXiv:gr-qc/0507014.
- [123] M. Campanelli, C. O. Lousto, P. Marronetti, Y. Zlochower: Accurate evolutions of orbiting black-hole binaries without excision, *Phys. Rev. Lett.* **96** (2006) 111101, arXiv:gr-qc/0511048.
- [124] J.G. Baker, J. Centrella, D. Choi, M. Koppitz, J. van Meter: Gravitational wave extraction from an inspiraling configuration of merging black holes, *Phys. Rev. Lett.* **96** (2006) 111102, arXiv:gr-qc/0511103.
- [125] M. Campanelli, C. O. Lousto, Y. Zlochower: The last orbit of binary black holes, *Phys. Rev. D* **73** (2006) 061501, arXiv:gr-qc/0601091.
- [126] J.G. Baker, J. Centrella, D. Choi, M. Koppitz, J. van Meter: Binary black hole merger dynamics and waveforms, *Phys. Rev. D* **73** (2006) 104002, arXiv:gr-qc/0602026.
- [127] F. Pretorius: Simulation of binary black hole spacetimes with a harmonic evolution scheme, *Class. Quant. Grav.* **23** (2006) S529-S552, arXiv:gr-qc/0602115.
- [128] J.A. Gonzalez, U. Sperhake, B. Brüggmann, M. Hannam, S. Husa: Supermassive kicks for spinning black holes, *Phys. Rev. Lett.* **98**, 091101 (2007), arXiv:gr-qc/0702052.
- [129] M. Campanelli, C. O. Lousto, Y. Zlochower, D. Merritt: Merger recoils and spin flips from generic black-hole binaries, arXiv:gr-qc/0701164.
- [130] T. Damour, E. Gourgoulhon, P. Grandclement: Circular orbits of corotating binary black holes: Comparison between analytical and numerical results, *Phys. Rev. D* **66**, 024007 (2002), arXiv:gr-qc/0204011.
- [131] A. Buonanno, G.B. Cook, F. Pretorius: Inspiral, merger and ring-down of equal-mass black-hole binaries, arXiv:gr-qc/0610122; Y. Pan et al.: A data-analysis driven comparison of analytic and numerical coalescing binary waveforms: nonspinning case, (2007), arXiv:0704.1964[gr-qc].
- [132] J. Baker, J. van Meter, S. McWilliams, J. Centrella, B. Kelly: Consistency of post-Newtonian waveforms with numerical relativity, arXiv:gr-qc/0612024.

-
- [133] A. Nagar, T. Damour, A. Tartaglia: Binary black hole merger in the extreme mass ratio limit, arXiv:gr-qc/0612096.
- [134] T. Damour, A. Nagar: Binary black hole merger waveforms in the extreme mass ratio limit, arXiv:gr-qc/0612151; T. Damour and A. Nagar: Faithful Effective-One-Body waveforms of small-mass-ratio coalescing black-hole binaries, arXiv:0705.2519 [gr-qc].
- [135] T. Damour, A. Nagar: Final spin of a coalescing black-hole binary: an Effective-One-Body approach, arXiv:0704.3550[gr-qc].
- [136] T. Damour, P. Jaranowski, G. Schäfer: On the determination of the last stable orbit for circular general relativistic binaries at the third post-Newtonian approximation, Phys. Rev. D **62** (2000) 084011, arXiv:gr-qc/0005034.
- [137] T. Damour: Coalescence of two spinning black holes: An effective one-body approach, Phys. Rev. D **64**, 124013 (2001), arXiv:gr-qc/0103018.
- [138] L. Blanchet, T. Damour, G. Esposito-Farèse, B.R. Iyer: Gravitational radiation from inspiralling compact binaries completed at the third post-Newtonian order, Phys. Rev. Lett. **93** (2004) 091101, arXiv:gr-qc/0406012.
- [139] M. Davis, R. Ruffini, W.H. Press, R.H. Price: Gravitational radiation from a particle falling radially into a schwarzschild black hole, Phys. Rev. Lett. **27**, 1466-1469 (1971).
- [140] M. Davis, R. Ruffini, J. Tiomno, F. Zerilli: Can synchrotron gravitational radiation exist?, Phys. Rev. Lett. **28**, 1352-1355 (1972).
- [141] T. Damour, P. Jaranowski, G. Schäfer: in preparation.
- [142] T. Damour, A. Nagar, P. Diener, D. Pollney, L. Rezzolla, R. Takahashi: in preparation.
- [143] L. Blanchet, G. Faye, B. R. Iyer, B. Joguet: Gravitational-wave inspiral of compact binary systems to 7/2 post-Newtonian order, Phys. Rev. D **65**, 061501 (2002) [Erratum-ibid. D **71**, 129902 (2005)], arXiv:gr-qc/0105099.
- [144] A. Buonanno, Y. Chen, T. Damour: Transition from inspiral to plunge in precessing binaries of spinning black holes, Phys. Rev. D **74**, 104005 (2006), arXiv:gr-qc/0508067.

